DEVELOPMENT OF PYTHON CODE FOR DECOHERENCE CORRECTED SURFACE HOPPING

A THESIS

submitted in partial fulfillment of the requirements

for the award of the dual degree of

Bachelor of Science-Master of Science

in

CHEMISTRY

by

MD. ELIOUS ALI MONDAL

(16111)

DEPARTMENT OF CHEMISTRY
INDIAN INSTITUTE OF SCIENCE EDUCATION AND RESEARCH BHOPAL
BHOPAL - 462066

April 2021

CERTIFICATE

This is to certify that **Md. Elious Ali Mondal**, BS-MS (CHEMISTRY), has worked on the project entitled **'Development of Python code for Decoherence Corrected Surface Hopping'** under my supervision and guidance. The content of this report is original and has not been submitted elsewhere for the award of any academic or professional degree.

April 2021 **Dr. Varadharajan Srinivasan**
IISER Bhopal

Committee Member	Signature	Date
Dr. Rati Sharma		
Dr. Varadharajan Srinivasan		
Dr. Y. Adithya Lakshmanna		

ACADEMIC INTEGRITY AND COPYRIGHT DISCLAIMER

I hereby declare that this project is my own work and, to the best of my knowledge, it contains no materials previously published or written by another person, or substantial proportions of material which have been accepted for the award of any other degree or diploma at IISER Bhopal or any other educational institution, except where due acknowledgement is made in the document.

I certify that all copyrighted material incorporated into this document is in compliance with the Indian Copyright Act (1957) and that I have received written permission from the copyright owners for my use of their work, which is beyond the scope of the law. I agree to indemnify and save harmless IISER Bhopal from any and all claims that may be asserted or that may arise from any copyright violation.

April 2021 **Md. Elious Ali Mondal**
IISER Bhopal

ACKNOWLEDGEMENT

MS-thesis is an important part of my scientific career and it is a beginning step towards my journey to become an independent scientific researcher. I would like to thank my supervisor Dr. Varadharajan Srinivasan for assigning me this insightful and conceptually rich project and also having critical discussions throughout. I would also like to thank Mr. Chakradhar Rangi for helping me understand the theory and code of this project, always having discussions with me whenever needed and guiding me through difficult situations.

Working in the AITG-lab would not have been possible without the help of seniors and labmates. I would like to thank Sayan Maity, Satyajit Mandal, Manish Rana, Shubhojit Banerjee and Jo Sony Kurian for always helping me out whenever I disturbed them.

My whole BS-MS journey would have been boring without my awesome friends. I would like to acknowledge Disha, Upasana, Sagar, Rana, Roy, Madhubani, Nihal, Subham, Mehul, Manoj, Divya, Amar, Subhashini, Aniket, Ranjini, Roushan, Prashant, Vidya, Kuldeep, Udit, Manish and everyone who made this 5-year a memorable experience.

My jourey in theoretical and computational field was initiated at my first summer and winter internship under Dr. Nirmal Ganguli. I would like to thank him for always cheering me and motivating me to do research.

Finally, whatever I am is because of my mother, father and brother. I would like to thank my family and friends for always supporting me.

Md. Elious Ali Mondal

ABSTRACT

If we irradiate molecules with UV or visible light, the electronic energy increases and the molecule adopts higher electronic states. Now when the molecule relaxes again to lower electronic states, the excess electronic energy must be transferred to nuclear motions, thus increasing the kinetic energy of nuclei. This high energy nuclei motion may lead the molecule to explore geometries in phase-space where there are near degeneracies between electronic states. These are regions of non-adiabaticity and cannot be treated within the Born-Oppenheimer approximation (BOA). To go beyond the BOA, we have to either adopt full quantum treatment of the system (i.e. the nuclei are also treated quantum mechanically, which is computationally very expensive), or resort to some other semi-classical approach which can account for the non-adiabaticity. One such approach, suggested by John Tully[1] called Fewest-Switches-Surface-Hopping (FSSH) has been able to successfully model the non-adiabatic effects in lots of molecules like photo-relaxation of nucleo-bases, photo-isomerizarion of azo-benzenes. An in-house python based Trajectory Surface Hopping code had already been developed earlier in the group by Chakradhar Rangi and Dr. Varadharajan Srinivasan[2]. This project was started with the vision to create an open-source and easily readable Non-adiabatic dynamics code. This thesis is an attempt at testing the code and adding functionalities like decoherence correction, Non-adiabatic coupling (NAC) calculation by orbital overlap, NAC for open-shell calculations, NAC-vector formulation and global phase correction.

LIST OF ABBREVIATIONS

BOA	Born-Oppenheimer Approximation
TSH	Trajectory Surface Hopping
FSSH	Fewest Switches Surface Hopping
NAC(T)	Non-Aidabatic Coupling (Term)
NACV	Non-Adiabatic Coupling Vector
IDC	Instantaneous Decoherence Correction
EDC	Energy based Decoherence Correction
DFT	Density Functional Theory
TDDFT	Time-Dependent DFT
LR-TDDFT	Linear Response TDDFT
CSF	Configuration State Functions
CIS	Configuration Interaction Singles
TDA	Tamm-Dancoff Approximation
MO	Molecular orbitals
GTO	Gaussian Type Orbitals

LIST OF SYMBOLS

$\hbar$	Planks constant
$\mathbf{r}$	Electronic coordinate vector(s)
$\mathbf{R}$	Nuclear coordinate vector(s)
$\mathbf{M}$	Nuclear mass
$\mathbf{m}$	Electronic mass
e^-	electron
g^p	Primitive gaussian
g^c	Contracted gaussian

CONTENTS

1. INTRODUCTION

Suppose we have an electron (e^-) in the ground state Ψ_0 of an infinite well. Now, lets start stretching the well. The stretching can be done in two extreme way:

(a) If we stretch **very slowly** (infinitesimal steps at a time), we will find that with change in the width of the well, the e^- is adapting to the change, still remaining in the ground state of the stretched well.

(b) If we stretch **very fast** (sudden stretch), the e^- won't be able to adapt quickly to the width change and we will find that the electronic wave-function will now be described as a superposition of eigenstates of the stretched well.

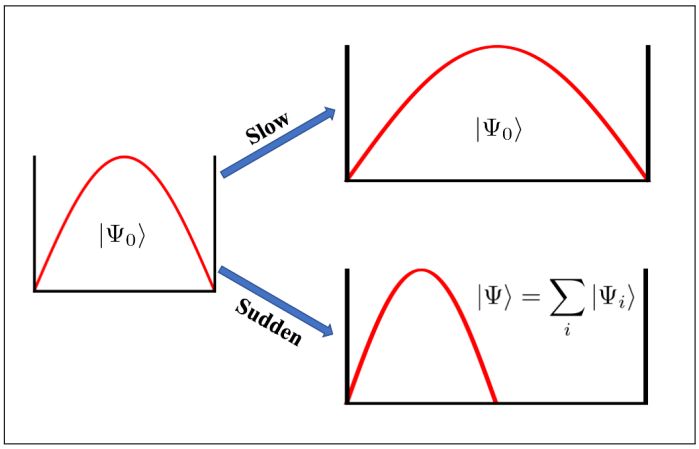

Fig. 1.1: Example of adiabatic(slow) and non-adiabatic(fast) changes

The example in **(a)** is a type of adiabatic change and that in **(b)** is a type of non-adiabatic change[3]. Lets now quantify how slow is adiabatic.

1.1 Adiabaticity in Quantum Mechanics

Lets consider a case where we prepare our system to be in the i^{th} eigenstate, ψ_i of the Hamiltonian $\hat{H}$. Then, with time, the system evolves according to time-dependent Schrödinger equation as:

$$i\hbar\frac{\partial}{\partial t}|\psi_i\rangle = \hat{H}|\psi_i\rangle \tag{1.1}$$

At each instant of time we can diagonalize the instantaneous Hamiltonian $\hat{H}(t)$,

$$\hat{H}(t)|\phi_j(t)\rangle = E(t)|\phi_j(t)\rangle \tag{1.2}$$

The time evolution of ψ can now be given as

$$|\psi(t)\rangle = \sum_j c_j(t)|\phi_j(t)\rangle \tag{1.3}$$

Putting eqn(1.3) in eqn(1.1) and rearranging a little will give us,

$$i\hbar\frac{\partial}{\partial t}\sum_j c_j(t)|\phi_j(t)\rangle = \hat{H}(t)\sum_j c_j(t)|\phi_j(t)\rangle \tag{1.4}$$

or,

$$i\hbar\sum_j\{\dot{c_j}(t)|\phi_j(t)\rangle + c_j(t)|\dot{\phi_j}(t)\rangle\} = \hat{H}(t)\sum_j c_j(t)|\phi_j(t)\rangle \tag{1.5}$$

Multiplying eqn(1.5) by $\langle\phi_k(t)|$, and doing little rearrangement will give,

$$i\hbar\dot{c_k}(t) = c_k(t)E_k(t) - i\hbar\sum_{j\neq k} c_j(t)\langle\phi_k(t)|\dot{\phi_j}(t)\rangle \tag{1.6}$$

Here $\dot{q}$ denotes time derivative of q. Eq(1.6) defines the evolution of our wavefunction (ψ) in terms of insteantaneous coefficients (c_k). Now lets take time derivative of eq(1.2),

$$\frac{\partial}{\partial t}\left(\hat{H}(t)|\phi_j(t)\rangle = E(t)|\phi_j(t)\rangle\right) \tag{1.7}$$

Expanding and multiplying with $\phi_k(t)$, for $k \neq j$, we get

$$\langle\phi_k|\dot{\hat{H}}|\phi_j\rangle + \langle\phi_k|\hat{H}|\dot{\phi}_j\rangle = \dot{E}_j\langle\phi_k|\phi_j\rangle + E_j\langle\phi_k|\dot{\phi}_j\rangle \tag{1.8}$$

Using $\langle\phi_k|\phi_j\rangle = \delta_{kj}$, we will get,

$$\langle\phi_k|\dot{\phi}_j\rangle = \frac{\langle\phi_k|\dot{\hat{H}}|\phi_j\rangle}{E_j - E_k} \tag{1.9}$$

Putting this in eq(1.6), we finally have,

$$\underbrace{i\hbar\dot{c}_k(t) = c_k(t)E_k(t)}_{\text{adiabatic part}} \underbrace{- i\hbar\sum_{j\neq k} c_j\frac{\langle\phi_k|\dot{\hat{H}}|\phi_j\rangle}{E_j - E_k}}_{\text{non-adiabatic part}} \tag{1.10}$$

The second part of eq(1.10) defines the measure of non-adiabaticity in the system. This can have significant magnitude if any of the following conditions are satisfied:

(a) Instantaneous wavefunctions are nearly degenerate, i.e. $E_j \approx E_k$

(b) The matrix element of rate of change of Hamiltonian in instantaneous eigenbasis is larger than the energy difference of the instantaneous eigenstates i.e. $|\langle\phi_k|\dot{\hat{H}}|\phi_j\rangle| \geqslant |E_j - E_k|/\hbar$.

If this part is significantly smaller than the first part of the equation, then we employ the **adiabatic approximation**,

$$i\hbar\dot{c}_k(t) \approx c_k(t)E_k(t) \tag{1.11}$$

In eqn(1.11), it can be clearly seen that if the Hamiltonian changes slowly, the system evolves in the same eigenstate. Now lets look at one of the fundamental approximations assumed in ground-state chemistry, the Born-Oppenheimer Approximation (BOA). In atoms and molecules, the nuclei are much heavier ($\sim \times 10^3$) and thus we assume, to the e^-, the nuclei is almost always stationary and that e^-'s can quickly adapt to any change in nuclear configuration. Thus, BOA is also a type of adiabatic approximation.

1.2 Born-Oppenheimer Approximation

For atoms and molecules, the Hamiltonian, in atomic units ($c = 1$, $\hbar = 1$, $m_e = 1$), can be written as;

$$\hat{H}(\mathbf{r},\mathbf{R}) = \overbrace{-\sum_A \frac{\nabla_A^2}{2M_A}}^{\text{Nuclear Kinetic energy}} \overbrace{-\sum_i \frac{\nabla_i^2}{2} + \sum_{i,j>i} \frac{1}{|\mathbf{r}_i - \mathbf{r}_j|} - \sum_{A,i} \frac{1}{|\mathbf{R}_A - \mathbf{r}_i|}}^{\text{Electronic part}} + \underbrace{\sum_{A,B>A} \frac{1}{|\mathbf{R}_A - \mathbf{R}_B|}}_{\text{Nucleus-Nucleus repulsion}} \tag{1.12}$$

Compressing the above equation via notations,

$$\hat{H}(\mathbf{r},\mathbf{R}) = \hat{T}_N + \hat{T}_e + \hat{V}_{ee} + \hat{V}_{eN} + \hat{V}_{NN} \tag{1.13}$$

Here $\hat{T}$ and $\hat{V}$ represents the kinetic energy and coulomb interaction operators respectively. The subscripts N and e correspond to nuclei and electrons. We now represent the electronic part of hamiltonian for fixed nuclear positions ($\mathbf{R}$), as H_e,

$$\hat{H}_e(\mathbf{r};\mathbf{R}) = \hat{T}_e + \hat{V}_{ee} + \hat{V}_{eN} \tag{1.14}$$

At any nuclear configuration $\mathbf{R}$, $\hat{H}_e$ can be diagonalised to give electronic eigenstates,

$$\hat{H}_e(\mathbf{r};\mathbf{R})|\Psi(\mathbf{r};\mathbf{R})\rangle = E_e(\mathbf{R})|\Psi(\mathbf{r};\mathbf{R})\rangle \tag{1.15}$$

Solving eqn(1.15) at different $\mathbf{R}$ will help us construct a surface of electronic energies as a function of nuclear coordinates and thus $E_e(\mathbf{R})$ is called a Potential Energy Surface (PES). Note the Ψ now depends parametrically on $\mathbf{R}$. Now we try to expand the total wavefunction of the molecule in electronic basis,

$$|\Phi(\mathbf{r},\mathbf{R})\rangle = \sum_j |\Psi_j(\mathbf{r};\mathbf{R})\rangle|\chi_j(\mathbf{R})\rangle \tag{1.16}$$

Here $|\chi_j(\mathbf{R})\rangle$ are the nuclear wavefunctions and they serve as the expansion coefficients. Dropping the variables to reduce complexity, the molecular

eigenvalue equation can now be written as,

$$\hat{H}\sum_j |\Psi_j\rangle|\chi_j\rangle = E\sum_j |\Psi_j\rangle|\chi_j\rangle \tag{1.17}$$

Multiplying with $\langle\Psi_i|$,

$$\sum_j \langle\Psi_i|\hat{H}|\Psi_j\rangle|\chi_j\rangle = E\sum_j \langle\Psi_i|\Psi_j\rangle|\chi_j\rangle \tag{1.18}$$

Denoting $\langle\Psi_i|\hat{H}|\Psi_j\rangle = H_{ij}$ and using orthonormality of electronic basis we have,

$$\sum_j \hat{H}_{ij}|\chi_j\rangle = E|\chi_i\rangle \tag{1.19}$$

Lets now look at the matrix element $\hat{H}_{ij}$,

$$\begin{aligned}\hat{H}_{ij} &= \langle\Psi_i|\hat{H}|\Psi_j\rangle \\ &= \langle\Psi_i|\hat{T}_N|\Psi_j\rangle + \hat{E}_e^i(\mathbf{R})\delta_{ij} + \hat{V}_{NN}\delta_{ij}\end{aligned} \tag{1.20}$$

Here $\hat{V}_{NN}$ is the nuclear repulsion energy operator. We have to now solve for the matrix element of nuclear kinetic energy operator in electronic basis,

$$\begin{aligned}(\hat{T_N})_{ij}|\chi_j\rangle &= \langle\Psi_i|\hat{T}_N|\Psi_j\rangle|\chi_j\rangle \\ &= -\frac{1}{2M_k}\langle\Psi_i|\nabla^2_{\mathbf{R}}|\Psi_j\rangle|\chi_j\rangle \\ &= -\frac{1}{2M_k}\langle\Psi_i|\nabla_{\mathbf{R}}.\nabla_{\mathbf{R}}|\Psi_j\rangle|\chi_j\rangle\end{aligned} \tag{1.21}$$

This can be expanded to show,

$$\begin{aligned}(\hat{T_N})_{ij}|\chi_j\rangle &= -\frac{1}{2M_k}\left[\langle\Psi_i|\nabla^2_{\mathbf{R}}|\Psi_j\rangle + 2\langle\Psi_i|\nabla_{\mathbf{R}}|\Psi_j\rangle\nabla_{\mathbf{R}} + \langle\Psi_i|\Psi_j\rangle\nabla^2_{\mathbf{R}}\right]|\chi_j\rangle \\ &= \left(-\Lambda_{ij} + T_N\delta_{ij}\right)|\chi_j\rangle\end{aligned} \tag{1.22}$$

where Λ_{ij} couples nuclear kinetic energy (slow degrees of freedom) with electronic eigenstates (fast degrees of freedom). This term is referred to as the

Non-Adiabatic Coupling (**NAC**) term,

$$\Lambda_{ij} = -\frac{1}{2M_k}(\langle\Psi_i|\nabla^2_{\mathbf{R}}|\Psi_j\rangle + 2\langle\Psi_i|\nabla_{\mathbf{R}}|\Psi_j\rangle\nabla_{\mathbf{R}}) \tag{1.23}$$

To know why this term is called the non-adiabatic coupling term, lets apply $\nabla_{\mathbf{R}}$ to eq(1.15),

$$\nabla_{\mathbf{R}}(\hat{H}_e|\Psi_j\rangle = E^j_e|\Psi_j\rangle) \tag{1.24}$$

Expanding and multiplying with $\langle\Psi_i|$, for $i \neq j$,

$$\langle\Psi_i|\nabla_{\mathbf{R}}\hat{H}_e|\Psi_j\rangle + \langle\Psi_i|\hat{H}_e\nabla_{\mathbf{R}}|\Psi_j\rangle = \nabla_{\mathbf{R}}E^j_e\langle\Psi_i|\Psi_j\rangle + E^j_e\langle\Psi_i|\nabla_{\mathbf{R}}|\Psi_j\rangle \tag{1.25}$$

Using $\langle\Psi_i|\Psi_j\rangle = \delta_{ij}$ and rearranging we get,

$$\langle\Psi_i|\nabla_{\mathbf{R}}|\Psi_j\rangle = \frac{\langle\Psi_i|\nabla_{\mathbf{R}}\hat{H}_e|\Psi_j\rangle}{E_j - E_i} \tag{1.26}$$

Using chain rule we can also derive eqn(1.26) from eqn(1.10). So, Λ_{ij} is the measure of non-adiabaticity in molecular systems. Now in BOA we set $\Lambda_{ij} = 0$ which leads to the decoupling of nuclear and electronic motions and eqn(1.19) becomes,

$$\begin{aligned} \sum_j \hat{H}_{ij}|\chi_j\rangle &= E|\chi_i\rangle \\ (T_N + E^i_e + E_{NN})|\chi_i\rangle &= E|\chi_i\rangle \end{aligned} \tag{1.27}$$

or we can say that under BOA,

$$E = T_N + E^i_e + E_{NN} = T_N + U \tag{1.28}$$

i.e. that the nuclei move under the average field of electrons on a single electronic PES, the U term in above eq(1.28). This approximation is mostly valid for ground-state phenomena near equilibrium geometries where the higher energy states are well separated from the ground state and the electronic motion is effectively decoupled from nuclear motion.

1.3 Breakdown of BOA

Consider the case of electronic excitation in ethylene (or any alkene). Ethylene has one C=C double bond in it's ground state. Due to its high energy, the double bond prevents any rotation along the C=C axis at room temperature. Now if we electronically excite the molecule, the C-C bond no longer has the double bond nature and the structure is free to rotate along the C-C bond. While the molecule undergoes dynamics in an excited state PES, the energy of ground state will increase as the structure deviates from its equilibrium geometry. With increase in ground state energy, during the dynamics we may encounter a structure at which the ground state is nearly degenerate with the excited state. From earlier section, we know that at this point we won't be able to apply BOA and that we now have to account for coupling of electronic and nuclear motions.

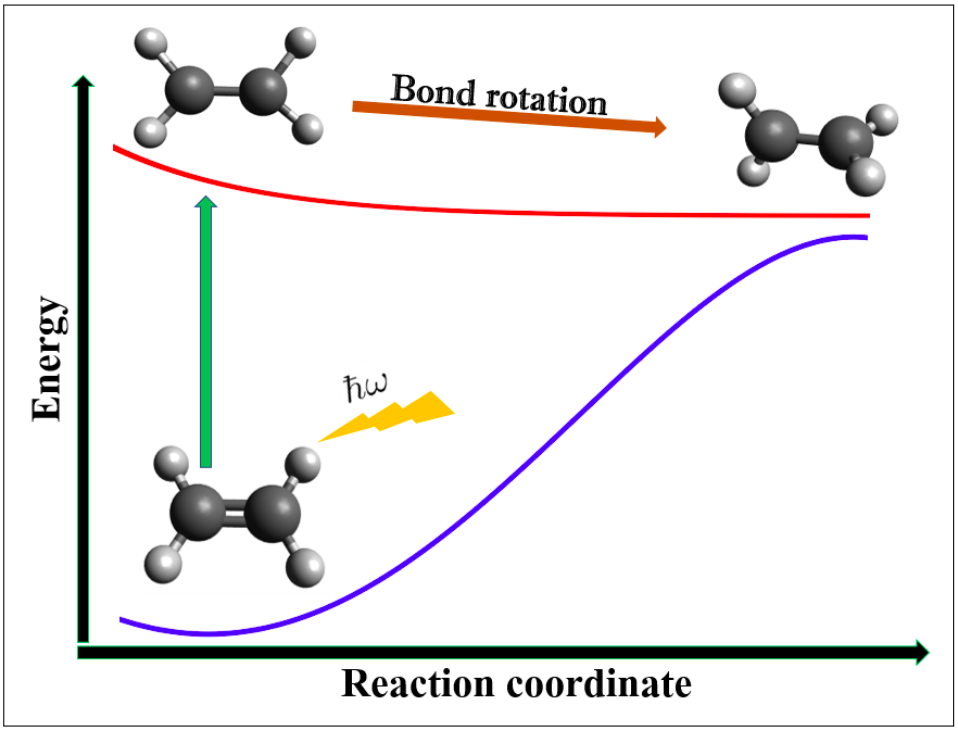

Fig. 1.2: Breakdown of BOA in ethylene. Blue and red represents the ground and exited state PES in the dynamics respectively.

1.4 Trajectory Surface Hopping

There are a lot of excited state phenomena where the BOA breaks down and we have to treat the system non-adiabatically to get more insight. Over the years, many such methods like AIMS (Ab-Initio Multiple spawning)[4], Ehrenfest Dynamics[5] and Trajectory Surface Hopping(TSH)[1], have been developed. These methods are able to capture scenarios of non-adiabaticity in excited states of molecules. TSH is based on the concept that we simulate an ensemble of different trajectories where the nuclei moves on a single PES but with a chance (to be decided by a stochastic algorithm) to hop to another surface near in energy. The average behaviour of this ensemble should be able to describe the overall non-adiabatic behaviour in the system. One such TSH approach, developed by Tully in 1990[1], called FSSH (Fewest Switches Surface Hopping) has been successful in describing lot of non-adiabatic processes. Our group has been working on a python based im-

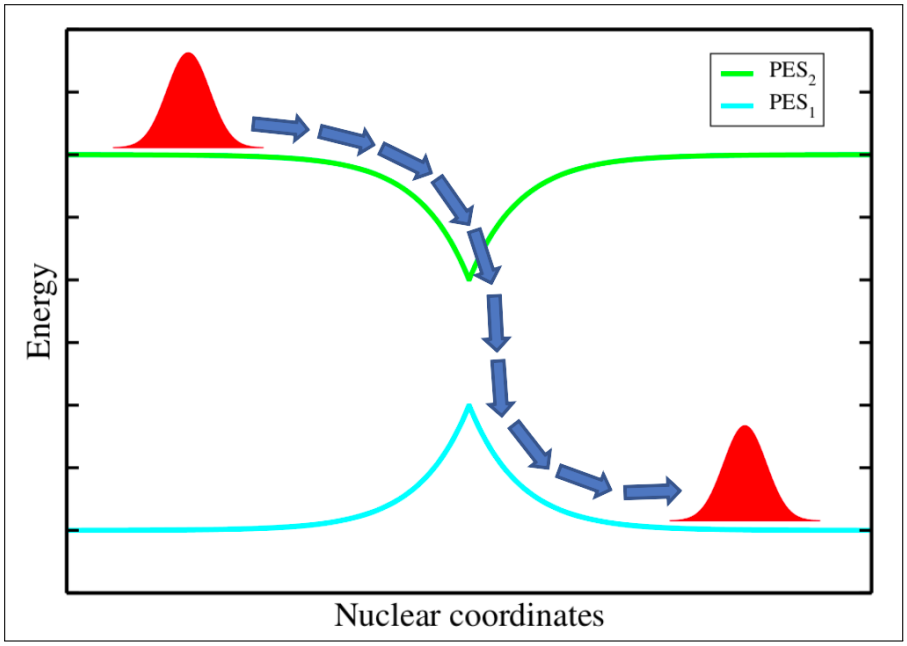

Fig. 1.3: The nuclear wavepacket switches the PES at strong coupling region in TSH.

plementation of FSSH non-adiabatic dynamics. Our python code essentially

functions as a wrapper carrying out the FSSH-dynamics using the NWChem code for first-principles excited state calculation. Herein we focus on testing the performance of the code as well as implementing new features such as electronic decoherence, a faster algorithm for NAC calculations and an extension to spin-polarised systems.

2. METHOD

The FSSH code has been developed within the LR-TDDFT (Linear Response Time Dependent Density Functional Theory) framework[2, 6]. We first provide a brief overview of LR-TDDFT and then move on to provide a brief theoretical summary of the FSSH along with ways to calculate the NACs and decoherence corrections.

2.1 Density Funcional Theory

There have been a lot of attempts in the quantum chemistry and condensed matter community to solve eq(1.15). The most notorious term in $\hat{H}_{e^-}$ is the e^--e^- repulsion term which makes the direct solution of eq(1.15) intractable for systems containing more than 3 or 4 e^-s. Since 1950's, Physicists and quantum chemist's have developed a lot of approximate techniques to deal with this term. Out of all these approaches, Density Functional Theory (DFT) has emerged to be one of the most successful theories[7]. Here we give a brief discussion about Hohenberg-Kohn theorems which are at the heart of DFT and the Kohn-Sham formalism[8] which has made DFT capable of being applied to solve real molecular problems.

2.1.1 Slater Determinant

For a moment, if we try to imagine some fictitious e^-s which have no interactions among themselves, the $\hat{H}_{e^-}$ just becomes,

$$\hat{H}_{e^-}^{non} = \sum_i -\frac{\nabla_i^2}{2} + \sum_A \sum_i \frac{1}{|\mathbf{r}_i - \mathbf{R}_A|} = \sum_i \hat{h}_i \tag{2.1}$$

Thus in case of non-interacting e^-s, the $\hat{H}_{e^-}^{non}$ is seperable into individual single-e^- hamiltonians $\hat{h}_i$. The $\hat{h}_i$ will give rise to single paricle orbitals

$$\hat{h}_i\phi_i = \epsilon_i\phi_i \tag{2.2}$$

Here ϵ_i are the single-particle orbital energies. Due to seperability of $\hat{H}_{e^-}^{non}$, the wavefunction of the whole non-interacting system can now be written as,

$$\Phi^H(\mathbf{r}_1, \mathbf{r}_2, ..., \mathbf{r}_N) = \phi_1(\mathbf{r}_1)\phi_2(\mathbf{r}_2)...\phi_N(\mathbf{r}_N) \tag{2.3}$$

This is sometimes also called the Hartree product and thats why Φ^H. This could be our simplest approximation for the wavefunction of an N-e^- system. But Φ^H has a basic problem of not being antisymmetric. Any fermionic wavefunction must be anti-symmetric with respect to change in fermionic coordinates, i.e.

$$\Phi(\mathbf{r}_1, .., \mathbf{r}_i, .., \mathbf{r}_j, .., \mathbf{r}_N) = -\Phi(\mathbf{r}_1, .., \mathbf{r}_j, .., \mathbf{r}_i, .., \mathbf{r}_N) \tag{2.4}$$

To make Φ^H antisymmetric, instead of taking simple product of ϕ_i, we construct a determinant out of those orbitals as follows[9],

$$\begin{aligned}\Phi(\mathbf{x}_1, \mathbf{x}_2, ..., \mathbf{x}_N) &= \frac{1}{\sqrt{N!}}\begin{vmatrix} \phi_1(\mathbf{x}_1) & \phi_2(\mathbf{x}_1) & ... & \phi_N(\mathbf{x}_1) \\ \phi_1(\mathbf{x}_2) & \phi_2(\mathbf{x}_2) & ... & \phi_N(\mathbf{x}_2) \\ \vdots & \vdots & \ddots & \vdots \\ \phi_1(\mathbf{x}_N) & \phi_2(\mathbf{x}_N) & ... & \phi_N(\mathbf{x}_N) \end{vmatrix} \\ &= \frac{1}{\sqrt{N!}}\sum_{n=1}^{N!}(-1)^{p_n}P_n\{\phi_1(\mathbf{x}_1)\phi_2(\mathbf{x}_2)...\phi_N(\mathbf{x}_N)\}\end{aligned} \tag{2.5}$$

Here P_n is the permutation operator and p_n represents the parity of permutation. Eq(2.5) is also known as a Slater determinant. This single Slater determinant formed out of single particle orbitals is our simplest guess for the many-body anti-symmetric wavefunction.

2.1.2 Hohenberg-Kohn Theorems

DFT is based on two, very simple theorems which were proved in 1964 by Pierre C. Hohenberg and Walter Kohn[7].

Theorem 1: *The external potential* $\boldsymbol{V}_{ext}$ *and hence the total energy* $\boldsymbol{E}_{tot}$ *is a unique functional of density* ρ*, i.e. there is a one to one relation between* $\boldsymbol{V}_{ext}$ *and* ρ

$$\rho \leftrightarrow \mathbf{V}_{ext} \tag{2.6}$$

Theorem 2: *The total energy will be minimised by the exact ground state density, i.e.*

$$\begin{aligned} E_{gs} &= E[\rho] \text{ for } \rho = \rho_{gs} \\ E_{gs} &< E[\rho] \text{ for } \rho \neq \rho_{gs} \end{aligned} \tag{2.7}$$

These two theorems help establishing the fact that electronic density ρ contains the same amount of information as the wavefunction Φ. Once we know the ground state density of the system, in principle we can determine any property of the system. The huge advantage of this fact is that, now the 3N dimensional problem just reduces to the problem of 3 dimensions. The problem is that we don't know how to determine this density and even if we determine the density, we don't know how the different properties depend on density.

2.1.3 Kohn-Sham formalism

In 1965, Walter Kohn and Lu Jeu Sham developed a procedure for finding the electronic density[8]. They assumed, for every interacting system, there exists a non-interacting system of the same density. The density of this non-interacting system is calculated in terms of single particle orbitals,

$$\rho(\mathbf{r}) = \sum_{i=1}^{N} |\phi_i(\mathbf{r})|^2 \tag{2.8}$$

where ϕ_i are obtained from single-particle schrödinger like equations,

$$\left[-\frac{\nabla^2}{2} + v_s[\rho](\mathbf{r})\right]\phi_j(\mathbf{r}) = \epsilon_j\phi_j(\mathbf{r}) \tag{2.9}$$

Here the single-particle Kohn-Sham potential $v_s[\rho]$ is given,

$$v_s[\rho] = v_{ext}[\rho] + v_H[\rho] + v_{xc}[\rho] \tag{2.10}$$

Here v_{ext}, v_H, v_{xc} are the external potential, Hartree potential (classical coulomb potential) and exchange-correlation potential respectively. v_{xc} describes the many-body effects and the exact analytical form of this term is not known till date. Since 1980's, many dependable approximations for v_{xc} have been developed. In practice, eq(2.9) is solved iteratively to get energy minimised single particle orbitals ϕ_j which inturn are used to reproduce the correct density of the interacting system.

2.2 Time Dependendent DFT

In the previous section, we attempted a solution to the stationary many body problem. The time-dependent version will be obtained by,

$$i\frac{\partial}{\partial t}\Phi(\mathbf{r}_1, ..., \mathbf{r}_N, t) = \hat{H}(t)\Phi(\mathbf{r}_1, ..., \mathbf{r}_N, t) \tag{2.11}$$

where

$$\hat{H}(t) = \hat{T} + \hat{V}_{ext}(t) + \hat{V}_{ee} \tag{2.12}$$

with

$$\hat{V}_{ext}(t) = \sum_{j=1}^{N} v_{ext}(\mathbf{r}_j, t) \tag{2.13}$$

Given any initial state Φ_{in}, the system evolves to a final state Φ_{fin} by following eq(2.11). Now to evolve the density ρ in time, we need some time-dependent version of Hohenberg-Kohn theorems.

2.2.1 Runge-Gross Theorem

In 1984, Erich Runge and E.K.U.Gross attempted to formalise a time-dependent version of DFT and came up with the following theorem[10, 11]:

Theorem 3: *If two N-e^- systems start from the same initial density but are subjected to two different time-dependent potentials, then the evolution of densities of these two systems will be different.* So, if we have two systems with same initital density n subjected to different time-dependent potentials V_1 and V_2 given any initial state Φ_0, there is a one to one correspondence between the time dependent potential and density,

$$\rho(\mathbf{r}, t) \leftrightarrow \mathbf{V}_{ext}(\mathbf{r}, t) \tag{2.14}$$

2.2.2 Van-Leeuwen Theorem

Now for practical purposes, we need a time dependent version of Kohn-Sham formalism. Van Leeuwen in 1999, provided us with a theorem which makes this possible[11, 12].

Theorem 4: *For every time-dependent density $\rho(\boldsymbol{r}, t)$ associated with a many-body system where the particle interaction is given by $w(|\boldsymbol{r}_1 - \boldsymbol{r}_2|)$ and the external potential by $v(\boldsymbol{r}, t)$, there exists a different many-body system with interaction $w'(|\boldsymbol{r}_1 - \boldsymbol{r}_2|)$ and potential $v'(\boldsymbol{r}, t)$ which reproduces the same density.*

So we can now have a time-dependent non-interacting system reproducing the same density evolution as the interacting system. The time-dependent single particle orbitals of the non-interacting system will be obtained by solving,

$$i\frac{\partial}{\partial t}\phi_j(\mathbf{r}, t) = \left[-\frac{\nabla^2}{2} + v_s(\mathbf{r}, t)\right]\phi_j(\mathbf{r}, t) \tag{2.15}$$

where v_s is defined similar to eqn(2.10) with just the difference being that it depends on the initial state of the interacting system Ψ_0 and the Kohn-sham

system Φ_0,

$$v_s[\rho, \Phi_0, \Psi_0](\mathbf{r}, t) = v_{ext}(\mathbf{r}, t) + v_H(\mathbf{r}, t) + v_{xc}[\rho, \Phi_0, \Psi_0](\mathbf{r}, t) \tag{2.16}$$

2.3 Linear Response TDDFT

If we apply a weak time-dependent perturbation to a system, to a good extent, we would be able to capture the response of the system with first order of perturbation. This is called linear response regime[2]. Let us start with a system, initially in the ground state Φ_0 and at time $t = t_0$, we switch ON the perturbation as follows,

$$v_{ext}(\mathbf{r}, t) = v_0(\mathbf{r}) + \theta(t - t_0)v_1(\mathbf{r}, t) \tag{2.17}$$

Here θ is the step function. The changed density can be expanded as

$$\rho(\mathbf{r}, t) = \rho_0(\mathbf{r}) + \rho_1(\mathbf{r}, t) + \rho_2(\mathbf{r}, t) + ... \tag{2.18}$$

ρ_0, ρ_1, ρ_2,... represents the ground state density, first order linear response, second order quadratic response and so on respectively. The linear response can be written as,

$$\rho_1(\mathbf{r}, t) = \int_{-\infty}^{t} dt' \int d\mathbf{r}' \chi(\mathbf{r}, t, \mathbf{r}', t')v_1(\mathbf{r}, t) \tag{2.19}$$

χ is the density-density response function given by,

$$\chi(\mathbf{r}, t, \mathbf{r}', t')v_1(\mathbf{r}, t) = -i\langle\Phi_0|[\hat{\rho}(\mathbf{r}, t - t'), \hat{\rho}(\mathbf{r})]|\Phi_0\rangle \tag{2.20}$$

The fourier transform of the response function in Lehmann representation is given by:

$$\chi(\mathbf{r}, \mathbf{r}', \omega) = \lim_{\eta \to 0} \sum_{n=1}^{\infty} \frac{\langle\Phi_0|\hat{\rho}(\mathbf{r})|\Phi_n\rangle\langle\Phi_n|\hat{\rho}(\mathbf{r}')|\Phi_0\rangle}{\omega - \Omega_n + i\eta} - \frac{\langle\Phi_0|\hat{\rho}(\mathbf{r}')|\Phi_n\rangle\langle\Phi_n|\hat{\rho}(\mathbf{r})|\Phi_0\rangle}{\omega + \Omega_n + i\eta} \tag{2.21}$$

Here, $\Omega_n = E_n - E_0$ corresponds to the n^{th} excitation of the many-body system. Now lets look at the response in the Kohn-Sham system.

$$\rho_1(\mathbf{r},t) = \int_{-\infty}^{t} dt' \int \chi_{ks}(\mathbf{r},t,\mathbf{r}',t') v_{1ks}(\mathbf{r}',t') \tag{2.22}$$

where χ_{ks} now represents the density-density response in the Kohn-Sham system. The effective perturbation to the Kohn-Sham system is given by,

$$v_{1ks} = v_1(\mathbf{r},t) + \int d\mathbf{r}' \frac{\rho_1(\mathbf{r}',t)}{|\mathbf{r}-\mathbf{r}'|} + \int_{-\infty}^{t} dt' \int d\mathbf{r}' f_{xc}(\mathbf{r},t,\mathbf{r}',t')\rho_1(\mathbf{r}',t') \tag{2.23}$$

where f_{xc} is known as the exchange-correlation kernel and it is defined as functional derivative of v_{xc},

$$f_{xc}(\mathbf{r},t,\mathbf{r}',t') = \frac{\delta v_{xc}[\rho](\mathbf{r},t)}{\delta\rho(\mathbf{r}',t')} \tag{2.24}$$

The frequency dependent response and KS-potential are,

$$\rho_1(\mathbf{r},\omega) = \int d\mathbf{r}' \chi_{ks}(\mathbf{r},\mathbf{r}',\omega) v_{1ks}(\mathbf{r}',\omega) \tag{2.25}$$

$$v_{1ks} = v_1(\mathbf{r},\omega) + \int d\mathbf{r}' \frac{\rho_1(\mathbf{r},t)}{|\mathbf{r}-\mathbf{r}'|} + \int d\mathbf{r}' f_{xc}(\mathbf{r},\mathbf{r}',\omega)\rho_1(\mathbf{r}',\omega) \tag{2.26}$$

The Kohn-Sham response function can be written as,

$$\chi_{ks}(\mathbf{r},\mathbf{r}',\omega) = \lim_{\eta\to 0^+} \sum_{i,j=1}^{\infty} (f_j - f_i) \frac{\phi_i(\mathbf{r})\phi_j^*(\mathbf{r})\phi_i^*(\mathbf{r}')\phi_j(\mathbf{r}')}{\omega - \omega_{ij} + i\eta} \tag{2.27}$$

f_i represents the occupation number of ith Kohn-Sham orbital and $\omega_{ij} = \epsilon_i - \epsilon_j$ is the difference in Kohn-Sham orbital energies. Equations (2.25), (2.26) and (2.27) can be written in spin-dependent form,

$$\rho_{1\sigma}(\mathbf{r},\omega) = \sum_{\sigma'} \int d\mathbf{r}' \chi_{ks,\sigma\sigma'}(\mathbf{r},\mathbf{r}',\omega) v_{1ks\sigma}(\mathbf{r}',\omega) \tag{2.28}$$

$$v_{1ks\sigma} = v_{1\sigma}(\mathbf{r},\omega) + \sum_{\sigma'}\int d\mathbf{r}'\frac{\rho_{1\sigma'}(\mathbf{r},t)}{|\mathbf{r}-\mathbf{r}'|} + \sum_{\sigma'}\int d\mathbf{r}' f_{xc,\sigma\sigma'}(\mathbf{r},\mathbf{r}',\omega)\rho_{1\sigma'}(\mathbf{r}',\omega) \tag{2.29}$$

$$\chi_{ks,\sigma\sigma'}(\mathbf{r},\mathbf{r}',\omega) = \delta_{\sigma\sigma'}\lim_{\eta\to 0^+}\sum_{i,j=1}^{\infty}(f_{j\sigma}-f_{i\sigma})\frac{\phi_{i\sigma}(\mathbf{r})\phi^*_{j\sigma}(\mathbf{r})\phi^*_{i\sigma}(\mathbf{r}')\phi_{j\sigma}(\mathbf{r}')}{\omega-\omega_{ij}+i\eta} \tag{2.30}$$

From the above equation we can clearly see, the poles of frequency dependent response function are the excitation energies of the many-body system. Using eq(2.27), and assuming KS-orbitals are real, Marc Casida[13, 14] obtained the following non-Hermitian eigenvalue equation,

$$\begin{bmatrix}\mathbf{A} & \mathbf{B}\\ \mathbf{B}^* & \mathbf{A}^*\end{bmatrix}\begin{bmatrix}\mathbf{X}\\ \mathbf{Y}\end{bmatrix} = \omega\begin{bmatrix}1 & 0\\ 0 & -1\end{bmatrix}\begin{bmatrix}\mathbf{X}\\ \mathbf{Y}\end{bmatrix} \tag{2.31}$$

The elements of $\mathbf{A}$ and $\mathbf{B}$ matrices are given by,

$$A_{ia,jb} = \delta_{ij}\delta_{ab}(\epsilon_a-\epsilon_i) + (ia|jb) + (ia|f_{xc}|jb) \tag{2.32}$$

$$B_{ia,jb} = (ia|bj) + (ia|f_{xc}|bj) \tag{2.33}$$

with

$$(ia|f_{xc}|bj) = \int d\mathbf{r}d\mathbf{r}'\phi^*_i(\mathbf{r})\phi_a(\mathbf{r})\frac{\delta^2 E_{xc}}{\delta\rho(\mathbf{r})\delta\rho(\mathbf{r}')}\phi^*_b(\mathbf{r}')\phi_j(\mathbf{r}') \tag{2.34}$$

If we assume f_{xc} to be frequency independent, the casida equation, eq(2.31) can be rewritten as,

$$C\mathbf{Z} = \Omega^2\mathbf{Z} \tag{2.35}$$

with

$$C = (\mathbf{A}-\mathbf{B})^{\frac{1}{2}}(\mathbf{A}+\mathbf{B})(\mathbf{A}-\mathbf{B})^{\frac{1}{2}} \tag{2.36}$$

and

$$\mathbf{Z} = (\mathbf{A}-\mathbf{B})^{\frac{1}{2}}(\mathbf{X}-\mathbf{Y}) \tag{2.37}$$

Eq(2.35) can be iteratively solved to get the many-body excitation energies. In FSSH, we need the excited state wavefunctions for computing the Non-adiabatic couplings. Tavernelli *et al.* proposed that within LR-TDDFT

framework, we can form auxiliary multideterminantal wavefunction from single excitations to compute the couplings[6].

$$|\Phi_n\rangle = \sum_{ia} C_{ia}|\Phi_i^a\rangle \tag{2.38}$$

2.4 Fewest Switches Surface Hopping

FSSH is the similar to *abinitio* molecular dynamics, but here along with the nuclear propagation we have to also consider the propagation of electronic wavefunction. Also, at regions of strong coupling, this PES can be changed.

2.4.1 Nuclear Propagation

In principle we may consider our intial electronic wavefunction to be superposition of different electronic states Φ_k,

$$\Psi(\mathbf{r};\mathbf{R}(t)) = \sum_k c_k(t)\Phi_k(\mathbf{r};\mathbf{R}(t)) \tag{2.39}$$

But generally we assume that our nuclei starts evolving on a single electronic PES E_k, with wavefunction $\Phi_k(\mathbf{r};\mathbf{R}(t))$. So we allow the nuclei to move along the gradient of this PES following Newtons equation of motion,

$$M_I\ddot{\mathbf{R}} = -\nabla E_k(\mathbf{R}(t)) \tag{2.40}$$

2.4.2 Electronic propagation

The electronic coefficients propagate according to eq(1.10). Using chain rule in eq(1.10), we can show,

$$i\hbar\dot{c}_k(t) = c_k(t)E_k(t) - i\hbar\sum_{j\neq k} c_j\mathbf{d}_{ij}.\dot{\mathbf{R}} \tag{2.41}$$

where we define the NAC-vector as,

$$\mathbf{d}_{kj} = \langle\Phi_k|\nabla_{\mathbf{R}}|\Phi_j\rangle \tag{2.42}$$

In density matrix notation we have

$$\rho_{kj} = c_k c_j^* \tag{2.43}$$

The diagonal elements of this matrix are referred to as the **populations** and off-diagonal elements are called **coherences**. The time derivative of the above eqn. is,

$$\dot{\rho}_{kj} = \dot{c}_k c_j^* + c_k \dot{c}_j^* \tag{2.44}$$

Putting eq(2.41) in the above we can see that the elements of density matrix evolve according to,

$$i\hbar\dot{\rho}_{kj} = \rho_{kj}(E_k(\mathbf{R}) - E_j(\mathbf{R})) - i\hbar \sum_l \left\{ \rho_{lj}\mathbf{d}_{kl}.\dot{\mathbf{R}} + \rho_{kl}\mathbf{d}_{lj}.\dot{\mathbf{R}} \right\} \tag{2.45}$$

and from here the populations evolve as,

$$\dot{\rho}_{kk} = -\sum_{l \neq k} 2\mathrm{Re}(\rho_{kl}^* \mathbf{d}_{kl}.\dot{\mathbf{R}}) = \sum_{l \neq k} \gamma_{kl} \tag{2.46}$$

Eq(2.45) is in general obeyed if the initial state is a mixed state and in case of a pure initial state, this boils down to eq(2.41). We have now propagated the nuclei and along with that also the electronic coefficients.

2.4.3 Hopping Probability

During the electronic propagation, as can be seen from eq(2.41) or eq(2.45), we have to calculate the NACs ($\mathbf{d}_{ij}$) and also the hopping probability. To understand how this hopping probability can be calculated, let's consider a case in which we simulate N trajectories in a two level system[1], with states $|1\rangle$ and $|2\rangle$. So inititally the number of trajectories in each trajectory is given by,

$$\begin{aligned} N_1^{in} &= \rho_{11}^{in} N \\ N_2^{in} &= \rho_{22}^{in} N \end{aligned} \tag{2.47}$$

Here the superscripts *in* and *fin* denotes initial and final conditions respectively. Now just after a very small time Δt, let the populations change

$$\begin{aligned} \rho_{11}^{in} &\rightarrow \rho_{11}^{fin} \\ \rho_{22}^{in} &\rightarrow \rho_{22}^{fin} \end{aligned} \tag{2.48}$$

For simplicity lets assume that $\rho_{11}^{fin} < \rho_{11}^{in}$ and $\rho_{22}^{fin} > \rho_{22}^{in}$. To maintain $N_1 + N_2 = N$, we must have, the number of trajectories switching from $|1\rangle \rightarrow |2\rangle$ greater than $|2\rangle \rightarrow |1\rangle$. To minimize the number of such switches, we can set the number of $|2\rangle \rightarrow |1\rangle$ switch to be 0, and the number of $|1\rangle \rightarrow |2\rangle$ switch to $(\rho_{11}^{fin} - \rho_{11}^{in})N$. Since initially, there are $\rho_{11}^{in}N$ number of trajectories in $|1\rangle$, the probability that one of these will switch during small Δt is,

$$P_{1\rightarrow 2} = \frac{\rho_{11}^{fin} - \rho_{11}^{in}}{\rho_{11}^{fin}} \approx \frac{\dot{\rho}_{22}^{fin}\Delta t}{\rho_{11}^{fin}} = \frac{\gamma_{21}\Delta t}{\rho_{11}^{fin}} \tag{2.49}$$

Thus for a two level system, we can define the probability of hopping from eq(2.49). Hop is decided by choosing a uniform random number $0 < \zeta < 1$ and hopping will only be allowed between states,

$$\begin{aligned} |1\rangle \rightarrow |2\rangle \text{ if, } \frac{\gamma_{21}\Delta t}{\rho_{11}^{fin}} > \zeta \\ |2\rangle \rightarrow |1\rangle \text{ if, } \frac{\gamma_{12}\Delta t}{\rho_{22}^{fin}} > \zeta \end{aligned} \tag{2.50}$$

In general, for systems with many electronic levels involved, the hopping probability is computed as,

$$\begin{aligned} P_{j\rightarrow k}(t) &= \frac{\text{change in population of k due to j}}{\text{population of j}} \\ &= max\left[0, \frac{\gamma_{kj}dt}{\rho_{jj}}\right] \end{aligned} \tag{2.51}$$

The hop $|j\rangle \rightarrow |k\rangle$ is allowed if,

$$\sum_{m=1}^{k-1} P_{j\rightarrow m} < \zeta < \sum_{m=1}^{k} P_{j\rightarrow m} \tag{2.52}$$

2.5 Internal Inconsistency in FSSH

Suppose we simulated N^T number of trajectories and at any time step of the FSSH simulation, if we have N^α in the electronic state α, then we should have[15] :

$$\frac{N^\alpha}{N^T} = \frac{1}{N^T}\sum_{j=1}^{N^T}\rho^j_{\alpha\alpha} \tag{2.53}$$

This is known to be the internal consistency of FSSH. Tully's FSSH algorithm shows internal inconsistencies due to overcoherence of different electronic populations. To understand this let us consider the Born-Huang ansatz (eq-1.16) for total wavefunction of the combined nuclei-electron system:

$$|\Psi\rangle = \sum_i |\chi_i\rangle|\phi_i\rangle \tag{2.54}$$

where the χ and ϕ are nuclear and electronic wavefunctions respectively. The density matrix will be given as,

$$|\Psi\rangle\langle\Psi| = \sum_{i,j} |\chi_i\rangle|\phi_i\rangle\langle\phi_j|\langle\chi_j| \tag{2.55}$$

From here, we can find the electronic density matrix to be

$$\sigma_{el} = \sum_{i,j}\langle\chi_j|\chi_i\rangle|\phi_i\rangle\langle\phi_j| \tag{2.56}$$

Now to bring out the electronic density matrix from this;

$$\begin{aligned}\sigma_{el} &= \sum_{i,j}\int |\mathbf{R}\rangle\langle\mathbf{R}||\Psi\rangle\langle\Psi|d\mathbf{R} \\ &= \sum_{i,j}\int \langle\chi_j|\mathbf{R}\rangle\langle\mathbf{R}|\chi_i\rangle|\phi_i\rangle\langle\phi_j|d\mathbf{R} \\ &= \sum_{i,j}\langle\chi_j|\chi_i\rangle|\phi_i\rangle\langle\phi_j|\end{aligned} \tag{2.57}$$

From eq(2.39), we can find the density matrix in FSSH as,

$$\sigma_{el} = \sum_{i,j} c_i c_j^* |\phi_i\rangle\langle\phi_j| \tag{2.58}$$

Comparing eqns (2.57) and (1.20), we can see that

$$c_i c_j^* = \langle\chi_j|\chi_i\rangle \tag{2.59}$$

Any region of strong coupling between the adiabatic states would cause the nuclear wavefunction to split up and there will be a nuclear wavepacket on each of these adiabatic surfaces. After some time, when these adiabats are far apart, there will be no interference between the seperated wavepackets i.e. $\langle\chi_j|\chi_i\rangle \to 0$. From eq(2.59), the term $c_i c_j^*$ should also diminish after the trajectory passes through the strong coupling region i.e. the electronic coefficients should also stop interfering. This does not happen in Tully's FSSH as the c_i's keep evolving according to eq(1.6) and the electronic interference does not vanish. This over-interfering of the electronic coefficients is what leads to overcoherence in FSSH.

2.6 Decoherence corrections

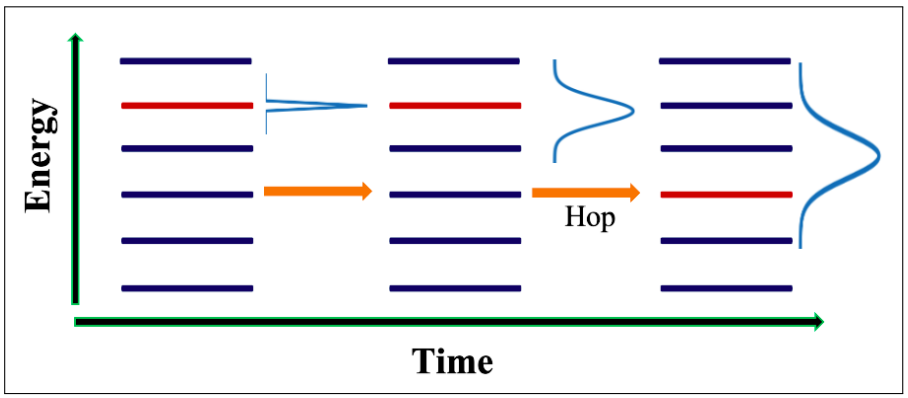

Fig. 2.1: Propagation of electronic wavefunction without decoherence correction. Red line represents the current electronic state[15]

From the above figure we can see that in standard FSSH, with propagation, the electronic wavefunction starts lagging compared to the current state. To correct for this overcoherence, some *ad-hoc* decoherence correction schemes have been developed over the years[16] and these are described below.

1. **Instantaneous Decoherence correction Simple(IDC-S) :** After each successful hop, the electronic wavefunction is re-initialised as a pure state in the current electronic state.

2. **Instantaneous Decoherence correction Accepted (IDC-A) :** If a hop is accepted, the wavefunction is made to collapse at the current state and if a hop is forbidden, the wavefunction is collapsed back to the current running state.

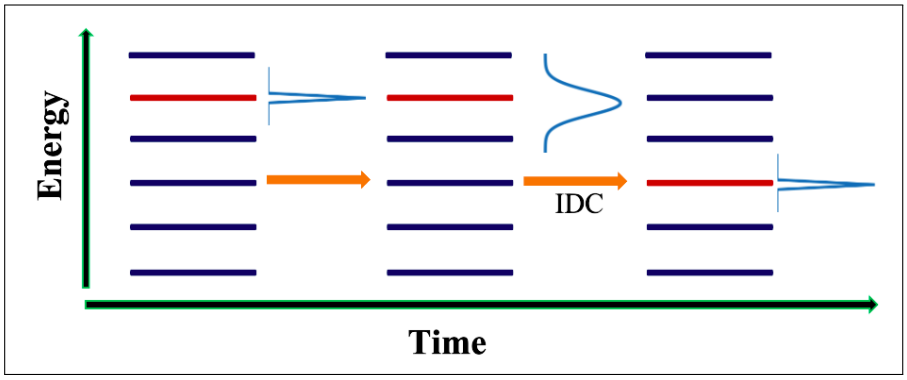

Fig. 2.2: Electronic wavefunction is forced to collapse at the current electronic state[15].

3. **Energy Based Decoherence Correction (EDC) :** Instead of instantaneous collapse, here we allow for decay of the electronic wavefunction to a particular state. If the current PES is of α and β represents other electronic states, then,

$$c'_\beta(t) = c_\beta(t) e^{\frac{-\Delta t}{\tau_{\beta\alpha}(t)}} \tag{2.60}$$

and the loss gets accumulated in the current state as:

$$c'_\alpha(t) = c_\alpha(t) \left[\frac{1 - \sum_{\beta \neq \alpha} |c'_\beta(t)|^2}{|c'_\alpha(t)|^2} \right]^{\frac{1}{2}} \tag{2.61}$$

$\tau_{\beta\alpha}$ is known as the decoherence time and Granucci *et al.*[15] suggested it to be:

$$\tau_{\beta\alpha}(t) = \frac{\hbar}{|E_\beta(t) - E_\alpha(t)|} \left(C + \frac{E_0}{E_{kin}} \right) \tag{2.62}$$

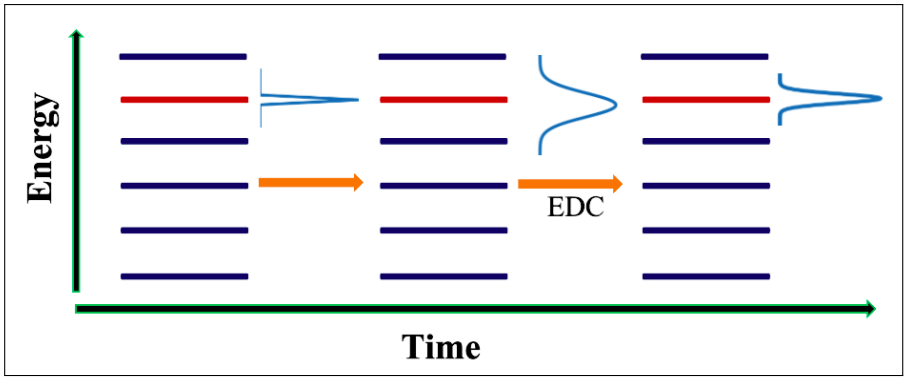

Fig. 2.3: After each nuclear step, the electronic coefficients are rescaled according to EDC[15].

Irrespective of whether any hop occur or not, after every nuclear time step, the electronic coefficients are rescaled.

2.7 Non-Adiabatic Coupling Term

The most important part of TSH is the calculation of the NAC term which actually accounts for the non-adiabaticity in our system. Over the years, many different formulas have been devised for calculating the time-dervative NAC term.

2.7.1 HST finite difference

The NAC is just the following time-derivative from eq(1.16),

$$\tau_{kj}(t) = \langle\psi_k|\frac{\partial}{\partial t}|\psi_j\rangle \tag{2.63}$$

Hammes Schiffer and Tully[17] devised a way to compute the above equation by combining finite differences and interpolation. The forward difference of eq(2.63) at t is,

$$\tau_{kj}(t) \approx \frac{\langle\psi_k(t)|\psi_j(t+\Delta t)\rangle - \langle\psi_k(t)|\psi_j(t)\rangle}{\Delta t} \tag{2.64}$$

The backward difference of eq(2.63) at $t + \Delta t$ is

$$\tau_{kj}(t+\Delta t) \approx \frac{\langle\psi_k(t+\Delta t)|\psi_j(t+\Delta t)\rangle - \langle\psi_k(t+\Delta t)|\psi_j(t)\rangle}{\Delta t} \tag{2.65}$$

Interpolating between these two time steps we get,

$$\tau_{kj}\left(t+\frac{\Delta t}{2}\right) \approx \frac{\tau_{kj}(t+\Delta t) + \tau_{kj}(t)}{2} \tag{2.66}$$

Putting eq(2.64) and eq(2.65) in eq(2.66) and using the orthonormality of wavefunctions at same time,

$$\tau_{kj}\left(t+\frac{\Delta t}{2}\right) \approx \frac{\langle\psi_k(t)|\psi_j(t+\Delta t)\rangle - \langle\psi_k(t+\Delta t)|\psi_j(t)\rangle}{2\Delta t} \tag{2.67}$$

So the calculation of NAC would require the wavefunction information at two consecutive time steps. We can also create a three point formula[18] using eq(2.67) to comute the NACs at time t instead of $t + \Delta t/2$. First we rewrite the above equation at time t,

$$\tau_{kj}(t) \approx \frac{\langle\psi_k(t-\Delta t/2)|\psi_j(t+\Delta t/2)\rangle - \langle\psi_k(t+\Delta t/2)|\psi_j(t-\Delta t/2)\rangle}{2\Delta t} \tag{2.68}$$

This, at $t - \Delta t/2$ becomes,

$$\tau_{kj}\left(t - \frac{\Delta t}{2}\right) \approx \frac{\langle\psi_k(t-\Delta t)|\psi_j(t)\rangle - \langle\psi_k(t)|\psi_j(t-\Delta t)\rangle}{2\Delta t} \tag{2.69}$$

and at $t - 3\Delta t/2$,

$$\tau_{kj}\left(t - \frac{3\Delta t}{2}\right) \approx \frac{\langle\psi_k(t-2\Delta t)|\psi_j(t)\rangle - \langle\psi_k(t)|\psi_j(t-2\Delta t)\rangle}{2\Delta t} \tag{2.70}$$

Through linear interpolation we can show,

$$\tau_{kj}(t) = \frac{3}{2}\tau_{kj}\left(t - \frac{\Delta t}{2}\right) - \frac{1}{2}\tau_{kj}\left(t - \frac{3\Delta t}{2}\right) \tag{2.71}$$

Putting eq(2.69) and eq(2.70) above,

$$\begin{aligned}\tau_{kj}(t) \approx &\frac{1}{4\Delta t}[3\langle\psi_k(t-2\Delta t)|\psi_j(t)\rangle - 3\langle\psi_k(t)|\psi_j(t-2\Delta t)\rangle \\ &- \langle\psi_k(t-2\Delta t)|\psi_j(t)\rangle + \langle\psi_k(t)|\psi_j(t-2\Delta t)\rangle]\end{aligned} \tag{2.72}$$

The advantage of this three point formula is that the NAC can be computed at the exact same nuclear time steps instead of midway. The disadvantage being that the wavefunction of three time steps are required. Now the excited state wavefunctions that we are referring to, are linear combination of Slater determinants that we obtain through a LR-TDDFT calculation. So for an electronic state k, the wavefunction we will be using is constructed from all possible singlet excitations within the chosen basis as,

$$|\Psi_k(t)\rangle = \sum_{ia} c_{ia}|\Psi_i^a(t)\rangle \tag{2.73}$$

Here $i, j \in$ **occupied** and $a, b \in$ **unoccupied** orbitals. These singly excited determinants are expanded as CSF's (configurational state functions) for closed shell cases, as they help conserve the spin symmetry.

$$|\Psi_i^a\rangle = \frac{1}{\sqrt{2}}\left(|\Psi_{i\alpha}^{a\beta}\rangle + |\Psi_{i\beta}^{a\alpha}\rangle\right) \tag{2.74}$$

Using eq(2.74), the first term in eq(2.67) can be expanded as[2, 19],

$$\begin{aligned}\langle\Psi_K(t)|\Psi_J(t+\Delta t)\rangle = \frac{1}{2}\sum_{ia}\sum_{jb} c_{ia}^{K*}(t)c_{jb}^{J}(t+\Delta t) \\ \Big\{\langle\Psi_{i\alpha}^{a\beta}(t)|\Psi_{i\alpha}^{a\beta}(t+\Delta t)\rangle + \langle\Psi_{i\alpha}^{a\beta}(t)|\Psi_{i\beta}^{a\alpha}(t+\Delta t)\rangle + \\ \Big\langle\Psi_{i\beta}^{a\alpha}(t)|\Psi_{i\alpha}^{a\beta}(t+\Delta t)\rangle + \langle\Psi_{i\beta}^{a\alpha}(t)|\Psi_{i\beta}^{a\alpha}(t+\Delta t)\rangle\Big\}\end{aligned} \tag{2.75}$$

These individual overlaps can be further broken down to the multiplication of $\alpha\alpha$ and $\beta\beta$ determinants to be described in section 2.6.

2.7.2 NAC through orbital overlap

The NAC calculation through determinant calculation described in the previous section requires the calculation of lots of determinant overlaps and it can be computationally costly if the number of CI-vectors needed to describe the excited state increases. An alternate formulation of NAC calculation has been done by Ryabinkin, Nagesh and Izamylov in 2015 when they broke down the determinant overlaps to just the overlap of molecular orbitals at different time steps[20]. This method led to a significnt reduction of NAC computation cost. The idea is that instead of taking the finite difference expansion of eq(2.63), we take the time-derivative of determinants itself.

$$\tau_{KJ} = \sum_{ijab}\left\{c_{ia}^{K*}\frac{\partial}{\partial t}c_{jb}^{J}\langle\Psi_i^a|\Psi_j^b\rangle + c_{ia}^{K*}c_{jb}^{J}\langle\Psi_i^a|\frac{\partial}{\partial t}|\Psi_j^b\rangle\right\} \tag{2.76}$$

The time derivative of the determinant can be expanded as,

$$\frac{\partial}{\partial t}|\Psi_j^b\rangle = \sum_{k\neq j}|\Psi_{jk}^{bk'}\rangle + |\Psi_j^{b'}\rangle \tag{2.77}$$

Here p' denotes that ϕ_p is replaced by the time derivative of ϕ_p. So we can now evaluate,

$$\langle\Psi_i^a\frac{\partial}{\partial t}|\Psi_j^b\rangle = \sum_{k\neq j}\langle\Psi_i^a|\Psi_{jk}^{bk'}\rangle + \langle\Psi_i^a|\Psi_j^{b'}\rangle \tag{2.78}$$

Using the orthonormality of molecular orbitals,

$$\langle \Psi_i^a | \Psi_j^{b'} \rangle = \delta_{ij} \langle \phi_a | \frac{\partial}{\partial t} \phi_b \rangle \tag{2.79}$$

and

$$\sum_{k \neq j} \langle \Psi_i^a | \Psi_{jk}^{bk'} \rangle = -P_{ij} \delta_{ab} \langle \phi_j | \frac{\partial}{\partial t} \phi_i \rangle \tag{2.80}$$

where P_{ij} depends on the ordering of MO's in the slater determinant and is given by,

$$\begin{aligned} |\Psi_i^a\rangle &= |..., \phi_{i-1}, \phi_a, \phi_{i+1}, ...| \rightarrow P_{ij} = 1 \\ |\Psi_i^a\rangle &= |..., \phi_{i-1}, \phi_{i+1}, ..., \phi_a| \rightarrow P_{ij} = (-1)^{|j-i|} \end{aligned} \tag{2.81}$$

So we have,

$$\langle \Psi_i^a \frac{\partial}{\partial t} | \Psi_j^b \rangle = \delta_{ij} \langle \phi_a | \frac{\partial}{\partial t} \phi_b \rangle - P_{ij} \delta_{ab} \langle \phi_j | \frac{\partial}{\partial t} \phi_i \rangle \tag{2.82}$$

Eqn(2.76) can now be written as,

$$\tau_{KJ} = \sum_{ia} c_{ia}^{K*} \frac{\partial}{\partial t} c_{jb}^J + \sum_{iab} c_{ia}^{K*} c_{jb}^J \langle \phi_a | \frac{\partial}{\partial t} \phi_b \rangle - \sum_{ija} P_{ij} c_{ia}^{K*} c_{jb} \delta_{ab} \langle \phi_j | \frac{\partial}{\partial t} \phi_i \rangle \tag{2.83}$$

Here the time-derivative matrix elements for $p \neq q$, are calculated as,

$$\langle \phi_p | \frac{\partial}{\partial t} \phi_q \rangle = \frac{\langle \phi_p(t) | \phi_q(t + \Delta t) \rangle}{\Delta t} \tag{2.84}$$

NAC calculation through the above method are faster than the determinant overlap calculation by an order of N_{occ}^3[20].

2.8 Non-Adiabatic Coupling Vector

Earlier in eq(1.26), we defined the NAC-Vector between any two states $|n\rangle$ and $|k\rangle$, for $k \neq j$,

$$\mathbf{d}_{kj} = \langle k | \nabla_{\mathbf{R}} | j \rangle \tag{2.85}$$

We now need to evaluate eq.(2.85) with $|n\rangle$ and $|k\rangle$ as determinants. Let $|k\rangle$ be a determinant formed from $\{\phi_i\}$ spin molecular orbitals, i.e.,

$$|k\rangle = |\phi_1\phi_2...\phi_m...\phi_N| \tag{2.86}$$

Applying $\nabla_{\mathbf{R}}$ on $|k\rangle$ we get,

$$\begin{aligned} \nabla_{\mathbf{R}}|k\rangle &= \nabla_{\mathbf{R}}|\phi_1\phi_2...\phi_m...\phi_N| \\ &= \sum_m |\phi_1\phi_2...(\nabla_{\mathbf{R}}\phi_m)...\phi_N| \\ &= \sum_m |k'_m\rangle \end{aligned} \tag{2.87}$$

where $|k'_m\rangle$ represents that ϕ_m in $|k\rangle$ is replaced by $\nabla_{\mathbf{R}}\phi_m$. So we have,

$$\mathbf{d}_{nk} = \langle n|\nabla_{\mathbf{R}}|k\rangle = \sum_m \langle n|k'_m\rangle \tag{2.88}$$

In general,

$$|n\rangle = \sum_{ia} c_{ia}|\Psi_{ia}\rangle \qquad \text{and} \qquad |k\rangle = \sum_{jb} c_{jb}|\Psi_{jb}\rangle \tag{2.89}$$

with $i, j \in$ **occupied** and $a, b \in$ **unoccupied** molecular orbitals. Eq(2.88) can now be expanded as

$$\begin{aligned} \mathbf{d}_{nk} &= \sum_{ia}\sum_{jb} c^*_{ia}\langle\Psi_{ia}|\nabla_{\mathbf{R}}|\Psi_{jb}\rangle c_{jb} \\ &= \sum_{ia}\sum_{jb}\sum_m c^*_{ia}\langle\Psi_{ia}|\Psi'_{jb,m}\rangle c_{jb} \end{aligned} \tag{2.90}$$

2.9 Overlap Calculations

In the previous sections, while calculating the NACs, we encounterd two main types of overlaps: overlap of determinants and overlap of molecular orbitals. We now dig deeper into how to carry out these overlap calculations.

2.9.1 Determinant overlap

Consider two determinant wavefunctions $|\Phi\rangle$ and $|\Phi'\rangle$ formed from spin molecular orbitals $\{\phi\}$ and $\{\phi'\}$ respectively. We assume that both these determinants have same number of α and β electrons[21]. The wavefunctions are,

$$\begin{aligned} |\Phi\rangle &= |\phi_1 ... \phi_{n_\alpha} \bar{\phi}_{n_\alpha+1} ... \bar{\phi}_N| \\ |\Phi'\rangle &= |\phi'_1 ... \phi'_{n_\alpha} \bar{\phi'}_{n_\alpha+1} ... \bar{\phi'}_N| \end{aligned} \tag{2.91}$$

Here n_α and N corresponds to number of α electrons and total number of electrons respectively. The orbitals with a bar ($\bar{\phi}$) are β spin orbitals. Also we have ordered the β electron orbitals after the α orbitals. This should be done by changing the sign every time any two orbitals are swaped. The overlap of these two determinants becomes[21],

$$\langle\Phi|\Phi'\rangle = \underbrace{\begin{vmatrix} \langle\phi_1|\phi'_1\rangle & \dots & \langle\phi_1|\phi'_{n_\alpha}\rangle \\ \vdots & \ddots & \vdots \\ \langle\phi_{n_\alpha}|\phi'_1\rangle & \dots & \langle\phi_{n_\alpha}|\phi'_{n_\alpha}\rangle \end{vmatrix}}_{\alpha\alpha} \times \underbrace{\begin{vmatrix} \langle\bar{\phi}_{n_\alpha+1}|\bar{\phi'}_{n_\alpha+1}\rangle & \dots & \langle\bar{\phi}_{n_\alpha+1}|\bar{\phi'}_N\rangle \\ \vdots & \ddots & \vdots \\ \langle\bar{\phi}_N|\bar{\phi'}_{n_\alpha+1}\rangle & \dots & \langle\bar{\phi}_N|\bar{\phi'}_N\rangle \end{vmatrix}}_{\beta\beta} \tag{2.92}$$

To calculate this determinant, we need to be able to calculate the overlap between molecular orbitals i.e. $\langle\phi|\phi'\rangle$.

2.9.2 Molecular orbital overlap

The MO's are localised over all atoms and they can be represented as the linear combination of atom centered orbitals[22].

$$|\phi\rangle = \sum_{I=1}^{N_A} \sum_c D_{Ic} |\tilde{g}_I^c(\mathbf{R}_I)\rangle \tag{2.93}$$

The $|\tilde{g}_I^c\rangle$ are atom centered orbitals and these are in turn linear combination of atom centered 3D primitive gaussian type functions $|\tilde{g}_p\rangle$,

$$|\tilde{g}^c\rangle = \sum_{i=1}^{L_c} d_i |\tilde{g}_p\rangle \tag{2.94}$$

The $|\tilde{g}^c\rangle$ are sometimes also referred to as contracted gaussians as $|\tilde{g}_p\rangle$ are contracted to look like Hydrogen like orbitals. Now these 3D primitive gaussians can be represented as cartesian and spherical gaussians. Currently we have implemented cartesian gaussians as cartesian gaussians. These have simplified expressions for evaluating molecular integrals. Multiplying two 3D primitive cartesian gaussians(G_{ikm} and G_{jln}) produces another gaussian distribution which can be easily shown by the gaussian product rule(appendix-A,[22]),

$$\Omega_{ab}(\mathbf{r}) = G_{ikm}(\mathbf{r}, a, \mathbf{A}) G_{jln}(\mathbf{r}, b, \mathbf{B}) \tag{2.95}$$

The integral over this resulting distribution becomes easy with the help of Hermite gaussians which have the form(appendix-B,[22]),

$$\Lambda_t(x, p, P_x) = \frac{\partial^t}{\partial^t_{P_x}} e^{-p x_P^2} \tag{2.96}$$

The integrals over hermite gaussians just turns out to be,

$$\int_{-\infty}^{+\infty} \Lambda_t(x) dx = \delta_{t0} \sqrt{\frac{\pi}{p}} \tag{2.97}$$

McMurchie-Davidson scheme for overlap integral

The gaussian overlap can be expanded as [2, 22],

$$\Omega_{ij} = \sum_{t=0}^{i+j} E_t^{ij} \Lambda_t \tag{2.98}$$

The expansion coefficients E_t^{ij} can be obtained by the recursion,

$$E_t^{i+1,j} = \frac{1}{2p}E_{t-1}^{ij} + X_{PA}E_t^{ij} + (t+1)E_{t+1}^{ij} \tag{2.99}$$

$$E_t^{i,j+1} = \frac{1}{2p}E_{t-1}^{ij} + X_{PB}E_t^{ij} + (t+1)E_{t+1}^{ij} \tag{2.100}$$

$$E_0^{00} = K_{ab}^x \tag{2.101}$$

$$E_t^{ij} = 0, \qquad t < 0 \text{ or } t > i + j \tag{2.102}$$

2.9.3 Common Computing Architecture (CCA) convention

NWChem[23] uses CCA[24] standard for calculating normalisation constant of basis elements. Since we use NWChem as our electronic structure code, we have also adopted the CCA normalisation standard. In this convention, the *x,y* and *z* components of a cartesian shell will be multiplied by,

$$\frac{1}{N} = \sqrt{\frac{(2i-1)!!(2j-1)!!(2k-1)!!}{(2i+2j+2k-1)!!}} \tag{2.103}$$

Here $i + j + k$ is the total angular momentum of the given orbital. This is done to normalise the orbitals along the cartesian axes to be 1.

2.9.4 Overlap calculation for NACV

In the calculation of NACV's, we came across matrix element of the form $\langle\phi_n|\vec{\nabla}_{\vec{R}}|\phi_m\rangle$. If this is expressed in terms of primitive gaussians, it can be evaluated by McMurchie-Davidson scheme . First, lets try to break this into primitive gaussian overlaps.

$$\begin{aligned}\langle\phi_n|\nabla_{\mathbf{R}}|\phi_m\rangle &= \langle\phi_n| \sum_{I=1}^{N_{atoms}} \left(\frac{\partial}{\partial R_{Ix}}\hat{x} + \frac{\partial}{\partial R_{Iy}}\hat{y} + \frac{\partial}{\partial R_{Iz}}\hat{z}\right)|\phi_m\rangle \\ &= \sum_{I=1}^{N_{atoms}} \left\{\langle\phi_n|\frac{\partial\phi_m}{\partial R_{Ix}}\rangle\hat{x} + \langle\phi_n|\frac{\partial\phi_m}{\partial R_{Iy}}\rangle\hat{y} + \langle\phi_n|\frac{\partial\phi_m}{\partial R_{Iz}}\rangle\hat{z}\right\}\end{aligned} \tag{2.104}$$

We try to look at one of the terms in eq(2.104). So we expand the $|\phi\rangle$ as the sum of atom-centered gaussians,

$$|\phi_m\rangle = \sum_{I=1}^{N_{atoms}} \sum_{i=1}^{N_c^I} D_{Ii} |\tilde{g}_i^c(\vec{R}_I)\rangle \tag{2.105}$$

Here, $N_c^I \rightarrow$ number of contractions for I^{th} atom, $\tilde{g}_i^c(\vec{R}_I) \rightarrow \imath^{th}$ contracted gaussian at $\vec{R}_I$ and $D_{Ii} \rightarrow$ the molecular orbital coefficient for $\tilde{g}_i^c$. Lets apply the x-component of nuclear gradient on ϕ_m,

$$\begin{aligned}
\nabla_x |\phi_m\rangle &= \sum_{I=1}^{N_{atoms}} \frac{\partial}{\partial R_{Ix}} |\phi_m\rangle \\
&= \sum_{I=1}^{N_{atoms}} \sum_{J=1}^{N_{atoms}} \sum_{i=1}^{N_c^J} D_{Ji} \frac{\partial}{\partial R_{Ix}} |\tilde{g}_i^c(\mathbf{R}_J)\rangle \\
&= \sum_{I=1}^{N_{atoms}} \sum_{J=1}^{N_{atoms}} \sum_{i=1}^{N_c^J} D_{Ji} \delta_{IJ} \frac{\partial}{\partial R_{Ix}} |\tilde{g}_i^c(\mathbf{R}_J)\rangle \\
&= \sum_{I=1}^{N_{atoms}} \sum_{i=1}^{N_c^I} D_{Ii} \frac{\partial}{\partial R_{Ix}} |\tilde{g}_i^c(\mathbf{R}_I)\rangle
\end{aligned} \tag{2.106}$$

Using eq(2.106) and expanding $\langle\phi_n|$ into atom-centered contracted gaussians, eq(2.104) can now be written as,

$$\langle\phi_n|\nabla_{\mathbf{R}}|\phi_m\rangle = \sum_{I=1}^{N_{atoms}} \sum_{i=1}^{N_c^I} \sum_{J=1}^{N_{atoms}} \sum_{j=1}^{N_c^J} D_{Ii}^* \langle\tilde{g}_i^c(\mathbf{R}_I)|\nabla_{\mathbf{R}}|\tilde{g}_j^c(\mathbf{R}_J)\rangle D_{Jj} \tag{2.107}$$

When expanded in terms of primitive gaussins, this boils down to evaluating the following distribution function,

$$\begin{aligned}
G_{ikm}\nabla_{\mathbf{A}} G_{jln} = (G_i \frac{\partial G_j}{\partial A_x})(G_k G_l)(G_m G_n)\hat{x} + (G_i G_j)(G_k \frac{\partial G_l}{\partial A_y})(G_m G_n)\hat{y} \\
+ (G_i G_j)(G_k G_l)(G_m \frac{\partial G_n}{\partial A_z})\hat{z}
\end{aligned} \tag{2.108}$$

Representing $G_i G_j = \Omega^x_{ij}$ and using eq(A.5), we can rewrite eq(2.108) as,

$$\begin{aligned} G_{ikm}\nabla_{\mathbf{A}} G_{jln} = &(2a\Omega^x_{i,j+1} - i\Omega^x_{i,j-1})\Omega^y_{kl}\Omega^z_{mn}\hat{x} \\ &+ \Omega^x_{ij}(2a\Omega^y_{k,l+1} - l\Omega^y_{k,l-1})\Omega^z_{mn}\hat{y} \\ &+ \Omega^x_{ij}\Omega^y_{kl}(2a\Omega^z_{m,n+1} - n\Omega^z_{m,n-1})\hat{z} \end{aligned} \tag{2.109}$$

2.10 Global phase correction

Diagonalising the electronic hamiltonian at each nuclear time step can buid up some arbitrary phase in the electronic wavefunctions due to the numerical approximation in the diagonalisation algorithm. This phase factor could be build up at two levels, the phase factor build in excited state wavefunction during solving the Casida equation (eq-2.31) and the phase factor developed in the molecular orbitals during solving the Kohn-Sham equations (eq-2.9). To prevent any such arbitrary phase development we have tried applying the global phase correction (GPC) to the NAC calculations.

1. For correcting the excited state wavefunctions, at each nuclear time step we calculate the diagonal elements of adiabatic wavefunction at current and previous time step. If any of the diagonal elements come out to be negative, then we change sign for the CI-vectors corresponding to that eigenstate.

$$\begin{aligned} \langle \Phi_i(t) | \Phi_i(t+\Delta t) \rangle < 0 \rightarrow -c_i(t+\Delta t) \\ \langle \Phi_i(t) | \Phi_i(t+\Delta t) \rangle \geqslant 0 \rightarrow c_i(t+\Delta t) \end{aligned} \tag{2.110}$$

2. For correction at MO level, We evaluate the molecular overlap matrix(**MOM**) and this matrix is then rounded (**MOMr**). The elements of **MOMr** will thus be 0,+1 or -1. This matrix is like a signed permutation matrix. The **MOM** will now be permuted according to **MOMr**

$$\begin{aligned} \mathbf{MOMr}_{ij} < 0 \rightarrow -\mathbf{MOM}_{ij} \\ \mathbf{MOMr}_{ij} \geqslant 0 \rightarrow \mathbf{MOM}_{ij} \end{aligned} \tag{2.111}$$

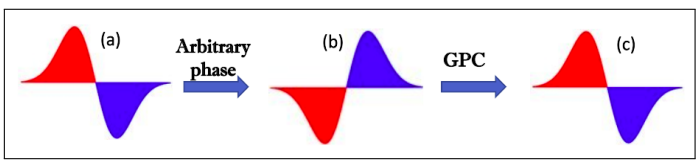

Fig. 2.4: Initial wavefunction (a), develops arbitrary phase in (b) and this is corrected by GPC in (c).

2.11 The algorithm of FSSH

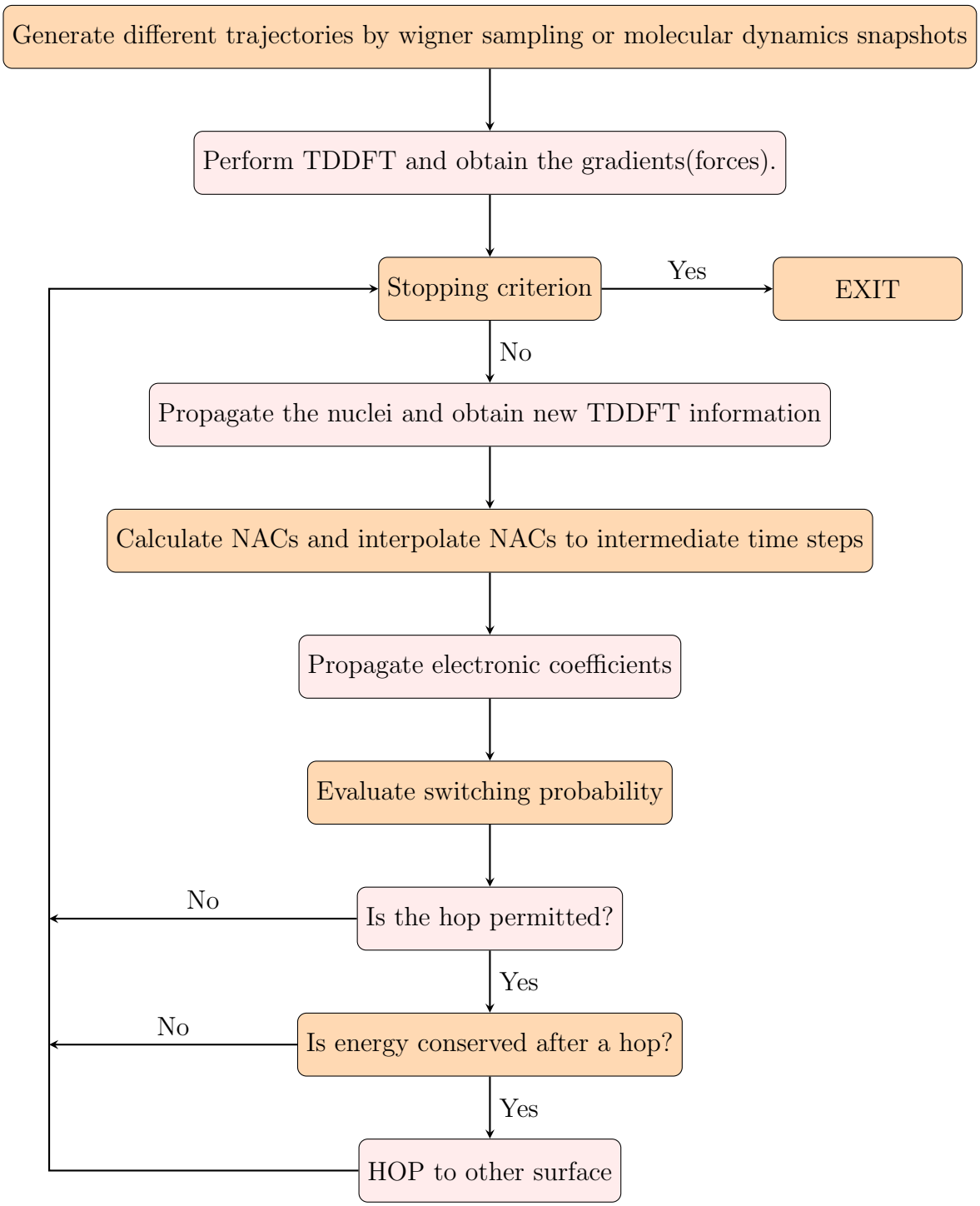

3. RESULTS

The tests for Non-adiabatic coupling (NACs) and Decoherence correction in our code are presented here. All the DFT and LR-TDDFT calculations were performed in NWChem-7.0.0[23]. In our code, we have presently implemented and done tests with the NAC formula by Hammes Schiffer and Tully (HST)[17] which is given by eq(2.67).

3.1 NAC testing

For testing of our HST implementation of NACs, we simulated a trajectory of N_2 for 100fs with a nuclear time step of 0.5fs and electronic time step of 0.0005fs in Newton-X[25], an already existing code for doing Non-adiabatic dynamics. For calculation of LR-TDDFT excitation energies and gradients, we chose 6-31G* basis set and B3LYP as the functional in Turbomole-2.0[26, 27]. This simulation was done on a single adiabatic surface of S_2 (2^{nd} singlet excited state) with the hopping turned off. We choose to examine the NACs between S_3 nd S_4 as these are the states which show frequent regions of avoided crossing in the simulation. As can be seen for fig(3.2) and fig(3.3), the positions of strong NAC regions are predicted to be same in both our code as well as Newton-X, but the signs and the magnitudes are not matching. Applying the global phase correction improves the agreement but still there are differences of magnitudes and signs in some regions.

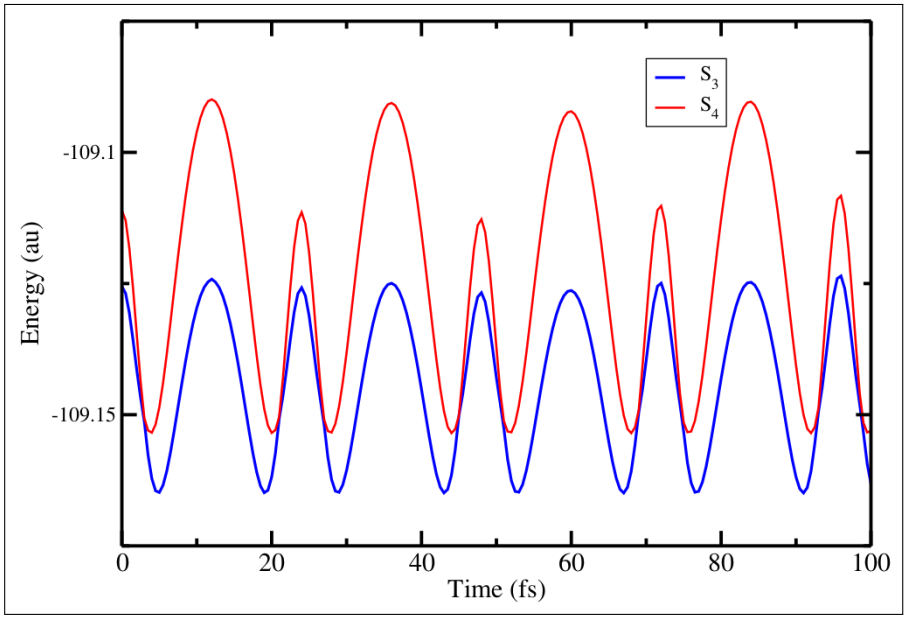

Fig. 3.1: Energies of S_3 and S_4 in the Newton-X simulation

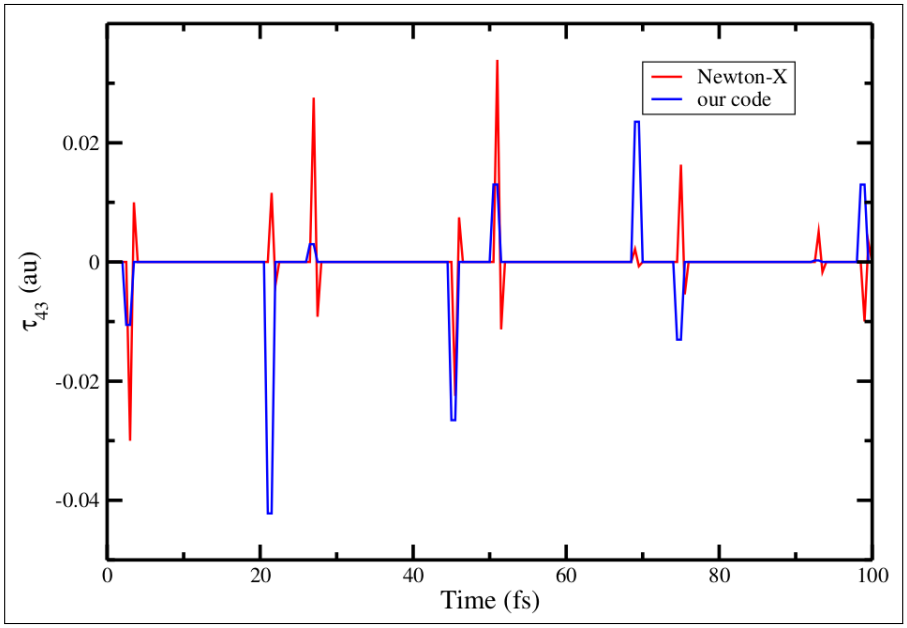

Fig. 3.2: NAC comparison of our NAC(HST) implementation and that from Newton-X. τ_{43} = NAC between S_3 and S_4

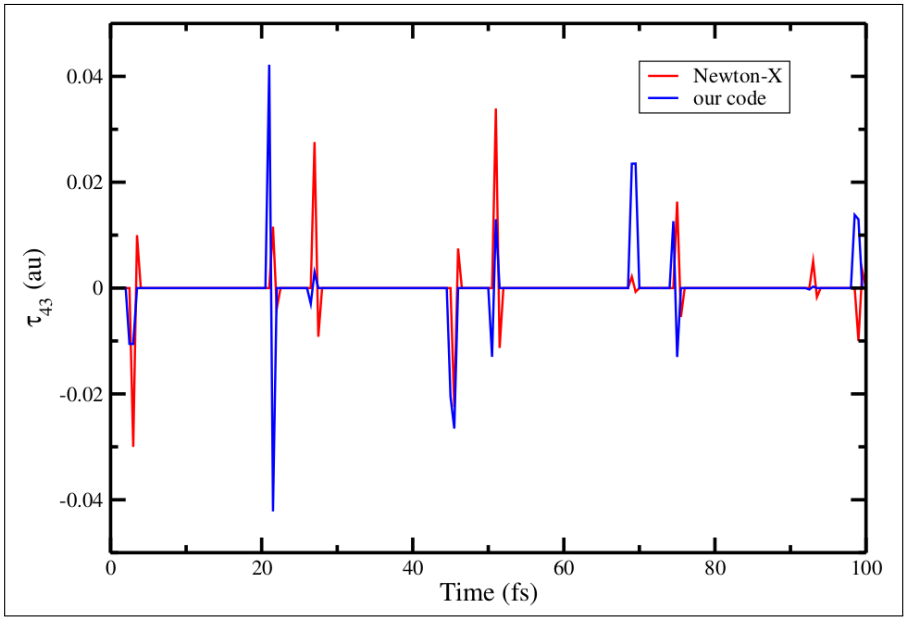

Fig. 3.3: NAC comparison of our NAC(HST) implementation and that from Newton-X after global phase correction. τ_{43} = NAC between S_3 and S_4

3.2 Decoherence correction (EDC) testing

In this section, we test for the effect of decoherence in our code. An ensemble of 65 trajectories of Ethylene were simulated once without any decoherence correction and once with EDC. The initial conditions were sampled using Wigner Sampling at 298K. For DFT and LR-TDDFT calculations, 6-31G* was used as the basis set with B3LYP as the functional. The nuclear time step was taken to be 0.5fs and the electronic time step was taken to be 0.00001fs with the total time for simulation as 100fs. In the TSH dynamics, the electronic wavefunction was taken to be expanded in 5 adiabatic states (1 ground state + 4 excited states). The 2^{nd} excited state (S_2) was taken as the initial sate as it was the first bright state. The result of both the simulations are presented below. To get a measure of internal inconsistency, we calculate the standard deviation(σ) of the electronic population of $S_2(\rho_{22})$ from the fraction of trajectories in $S_2(f_{22})$.

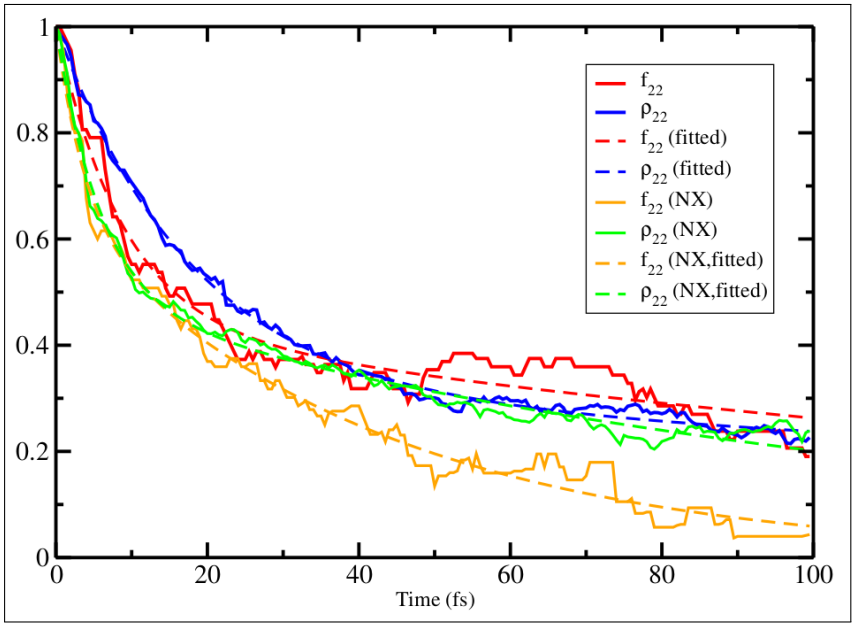

Fig. 3.4: No decoherence applied

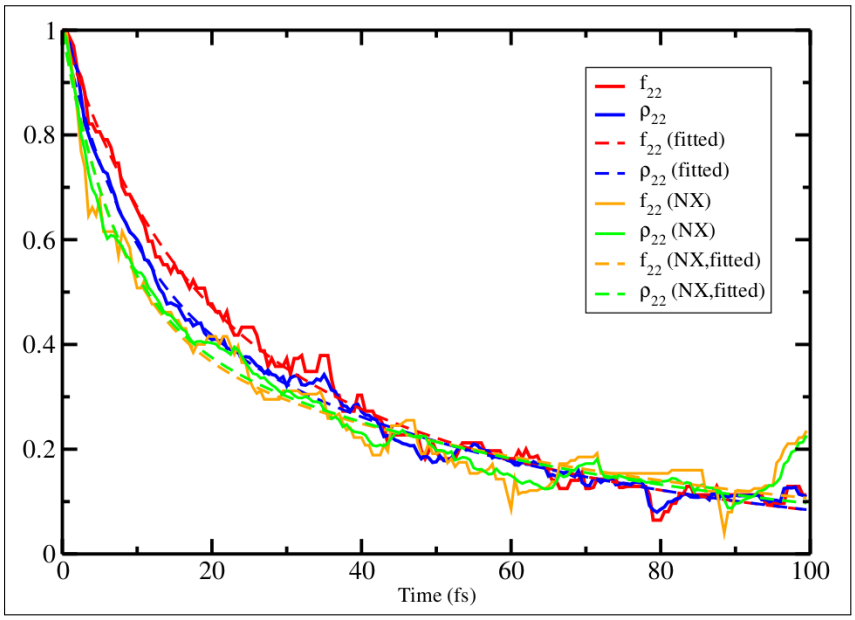

Fig. 3.5: EDC applied

$$\sigma = \sqrt{\frac{\sum(f_{22} - \rho_{22})^2}{N_{tsteps}}} \tag{3.1}$$

The standard deviation are,

	σ(our code)	σ(NX)
No Decoherence	0.0608	0.0024
with EDC	0.0332	0.0004

To get a measure of how the decay time scales are predicted by both schemes, the curves are fitted with biexponential function of the form

$$f(x) = ae^{-bx} + (1-a)e^{-cx} \tag{3.2}$$

Here the two time scales would be:

$$\tau_1 = \frac{1}{b} \text{ and } \tau_2 = \frac{1}{c} \tag{3.3}$$

The following are the results obtained:

1. Without decoherence

	a	$\tau_1(fs)$	$\tau_1(fs)$(NX)	$\tau_2(fs)$	$\tau_2(fs)$(NX)
f_{22}	0.443	200.000	41.525	8.850	3.719
ρ_{22}	0.315	333.333	114.056	17.857	5.926

2. With EDC

	a	$\tau_1(fs)$	$\tau_1(fs)$(NX)	$\tau_2(fs)$	$\tau_2(fs)$(NX)
f_{22}	0.533	53.763	71.407	13.333	7.608
ρ_{22}	0.545	53.476	62.895	8.475	7.064

The following are the observations form the tables presented above:

1. There is internal inconsistency in standard FSSH procedure as reflected by standard deviations and both code seem to improve the internal consistency after applying Energy based decoherence correction. Though, here the Newton-X performs much better compared to our code.

2. The time scales predicted by our code differs significantly from that in Newton-X when no decoherence correction was applied. Applying EDC, seems to have improved the agreement between our code and Newton-X, but they still differ.

The computational times for major time consuming steps of our code for a nuclear time step in a single trajectory ethylene FSSH simulation are given below.

Calculation type	Time taken (sec)
TDDFT	~ 19
Basis overlap	~ 0.2
NAC	~ 2
Electronic propagation	~ 136
Total	~ 158

Currently all the functionalities in our code are implemented serially and only the NWChem calculations can be done in parallel. The above calculation was done using a single core. For large molecules, the TDDFT calculation cost can be reduced by using more processors.

4. CONCLUSION

4.1 NAC testing

From the NAC test the following points can be observed,

1. The NACs in our are shooting up at the same nuclear points as the Newton-X code

2. The sign of the NACs don't agree at many points between our code and the Newton-X.

3. After applying global phase correction, we see that some of the NAC peaks have changed sign but it still doesn't match up with the Newtonx NACs.

The first observation indicates that our code is able to qualitatively define the non-adiabatic regions. The second point indicates that our code is still not able to quantitatively describe these regions. Also the global phase correction does not correct for the signs. Since the positions of the NACs are fine but the signs and magnitude are different, we have to compare the quantities which are used for the NAC calculation. Thus we should check for the MO-coefficients and also the CI-coefficient with the one produced by NewtonX. The signs of the NACs play an important role in the electronic propagation as in eq(1.6) and so to properly rely on the NAC calculation we are testing to make the signs of the NACs similar to that in NewtonX.

4.2 Decoherence testing

From the figures (3.4) and (3.5), it can be clearly observed that applying the decoherence correction does improve the internal consistency in FSSH and can also be verified by the standard deviation measures. Also the decoherence has improved the description of decay curves as can be seen from the lifetime fitted tables and the figures. While the decoherence improves the internal consistency within our code, when compared with a simulation with similar initial conditions in Newton-X, we can clearly see that the decay times produced by our simulation are very different than those of Newton-X. This can be traced to calculation of two different quantities,

1. The NAC calculation. As has been seen in the previous section, our code produces NACs with incorrect signs which inturn will cause error in electronic coefficient propagation (eq-1.6).

2. The electronic propagator. Our code is able to propagate the electronic coefficients only for very small electronic time steps. This is a problem if large systems are simulated. Also that it is working, only for very samll time step, indicates that there might be some error with the electronic propagation.

5. DISCUSSION

Our code[2] is still in its testing phase. At present the NACs are calculated through HST scheme, eq(2.67). Fast NAC calculation through orbital overlaps, eq(2.83) and NAC calculation for unrestricted cases has also been incorporated in the code but are yet to be tested. The algorithm for NAC-Vectors, eq(2.109) has been formulated and yet to be implemented as a code. As can be interpreted from the previous results, there are lot of testing and modifications to be done to the code. The following are the future plan possibilities:

1. Parallelisation of the code, on the trajectroy level and FSSH code functionalities like parallel computation of NACs.

2. To study processes like inter-system crossing, spin-orbit effects could also be included in the code.

3. For extending the TSH simulations to larger biological molecules, QM/MM implementaion has to be done.

4. The present code is only applicable to cartesian Pople basis. This can be extended to include other basis and also spherical basis sets.

Appendices

Appendix A

3D PRIMITIVE GAUSSIANS

The 3D primitive cartesian gaussians have the form,

$$\tilde{g}_p = G_{ijk}(\mathbf{r}, a, \mathbf{A}) = x_A^i y_A^j z_A^k e^{-ar_A^2} \tag{A.1}$$

Here $\mathbf{r}_A$, reperents the electronic coordinate $\mathbf{r}$ with respect to nuclear coordinate $\mathbf{R}$,

$$\mathbf{r}_A = \mathbf{r} - \mathbf{A} \tag{A.2}$$

The primitive gaussians can be factorised as:

$$G_{ijk}(\mathbf{r}, a, \mathbf{A}) = G_i(x, a, A_x) G_j(y, a, A_y) G_k(z, a, A_z) \tag{A.3}$$

where

$$G_i(x, a, A_x) = x_A^i e^{-ax_A^2} \tag{A.4}$$

These gaussians also have some nice properties. The first derivative:

$$\partial_{A_x} G_i = \frac{\partial G_i}{\partial A_x} = 2aG_{i+1} - iG_{i-1} = -\frac{\partial G_i}{\partial x} \tag{A.5}$$

Higher derivatives can be obtained as:

$$\frac{\partial^{q+1} G_i}{\partial A_x^{q+1}} = 2a\frac{\partial^q G_{i+1}}{\partial A_x^q} - i\frac{\partial^q G_{i-1}}{\partial A_x^q} \tag{A.6}$$

Denoting $G_i^q = \partial_{A_x}^q G_i$, we have the recursion

$$G_i^{q+1} = 2aG_{i+1}^q - iG_{i-1}^q \tag{A.7}$$

We have another simple recursion:

$$x_A G_i = G_{i+1} \tag{A.8}$$

For two gaussians centered at A and B, we have

$$e^{-ax_A^2} e^{-bx_B^2} = e^{-\mu X_{AB}^2} e^{-px_P^2} \tag{A.9}$$

Here

$$p = a + b \tag{A.10}$$

$$\mu = \frac{ab}{a+b} \tag{A.11}$$

$$P_x = \frac{aA_x + bB_x}{a+b} \tag{A.12}$$

$$X_{AB} = A_x - B_x \tag{A.13}$$

Sometimes we refer K_{ab}^x as the pre-exponential factor, where

$$K_{ab}^x = e^{-\mu X_{AB}^2} \tag{A.14}$$

If G_{ikm} and G_{jln} are two gaussians with exponents a,b are located at **A** and **B**, then we define:

$$\Omega_{ab}(\mathbf{r}) = G_{ikm}(\mathbf{r}, a, \mathbf{A}) G_{jln}(\mathbf{r}, b, \mathbf{B}) \tag{A.15}$$

We can factor this

$$\Omega_{ab}(\mathbf{r}) = \Omega_{ij}^x \Omega_{kl}^y \Omega_{mn}^z \tag{A.16}$$

Here

$$\Omega_{ij}^x = G_i(x, a, A_x) G_j(x, b, B_x) \tag{A.17}$$

Using the Gaussian product rule,

$$\Omega_{ij}^x = K_{ab}^x x_A^i x_B^j e^{-px_P^2} \tag{A.18}$$

Appendix B

HERMITE GAUSSIANS

The Hermite Gaussians of exponent p, centered on $\vec{P}$ are defined by

$$\Lambda_{tuv}(\vec{r}, p, \vec{P}) = \partial^t_{P_x} \partial^u_{P_y} \partial^v_{P_z} e^{-pr^2_P} \tag{B.1}$$

This can be further factorised as,

$$\Lambda_{tuv}(\vec{r}, p, \vec{P}) = \Lambda_t(x, p, P_x)\Lambda_u(y, p, P_y)\Lambda_v(z, p, P_z) \tag{B.2}$$

where

$$\Lambda_t(x, p, P_x) = \partial^t_{P_x} e^{-px^2_P} \tag{B.3}$$

The first derivative of an Hermite Gaussian is,

$$\frac{\partial \Lambda_t}{\partial P_x} = \Lambda_{t+1} = -\frac{\partial \Lambda_t}{\partial x} \tag{B.4}$$

We can show,

$$\Lambda_{t+1} = \partial^t_{P_x} \partial_{P_x} \Lambda_0 = 2p\partial^t_{P_x} x_P \Lambda_0 \tag{B.5}$$

using the commutator

$$[\partial^t_{P_x}, x_P] = -t\partial^{t-1}_{P_x} \tag{B.6}$$

we obtain,

$$\Lambda_{t+1} = 2p(x_P \Lambda_t - t\Lambda_{t-1}) \tag{B.7}$$

where we put $\Lambda_t = 0$ for $t < 0$. Using the above will give us the recursion relation,

$$x_P \Lambda_t = \frac{1}{2p}\Lambda_{t+1} + t\Lambda t - 1 \tag{B.8}$$

We can integrate the Hermite Gaussian as

$$\begin{aligned}\int_{-\infty}^{+\infty} \Lambda_t(x)dx &= \int_{-\infty}^{+\infty} \partial_{P_x}^t e^{-px_P^2} dx \\ &= \partial_{P_x}^t \int_{-\infty}^{+\infty} e^{-px_P^2} dx \\ &= \delta_{t0}\sqrt{\frac{\pi}{p}}\end{aligned} \tag{B.9}$$

This property is very important and can be efficiently used for the calculation of gaussian overlap distributions.

BIBLIOGRAPHY

(1) Tully, J. C. *The Journal of Chemical Physics* **1990**, *93*, 1061–1071.

(2) Rangi, C. *Development of a python code for modelling trajectory Surface Hopping on Ab-Initio Potential Energy Surface* **2020**, *Roll Number - 15200*, 1–57.

(3) Griffiths, D.; Griffiths, P., *Introduction to Quantum Mechanics*; Pearson international edition; Pearson Prentice Hall: 2005.

(4) Ben-Nun, M.; Quenneville, J.; Martınez, T. J. *The Journal of Physical Chemistry A* **2000**, *104*, 5161–5175.

(5) Li, X.; Tully, J. C.; Schlegel, H. B.; Frisch, M. J. *The Journal of chemical physics* **2005**, *123*, 084106.

(6) Curchod, B. F.; Rothlisberger, U.; Tavernelli, I. *ChemPhysChem* **2013**, *14*, 1314–1340.

(7) Hohenberg, P.; Kohn, W. *Physical review* **1964**, *136*, B864.

(8) Kohn, W.; Sham, L. J. *Physical review* **1965**, *140*, A1133.

(9) Szabo, A.; Ostlund, N. S., *Modern quantum chemistry: introduction to advanced electronic structure theory*; Courier Corporation: 2012.

(10) Runge, E.; Gross, E. K. *Physical Review Letters* **1984**, *52*, 997.

(11) Ullrich, C. A., *Time-dependent density-functional theory: concepts and applications*; OUP Oxford: 2011.

(12) Van Leeuwen, R. *Physical review letters* **1999**, *82*, 3863.

(13) Casida, M. E. In *Recent Advances In Density Functional Methods: (Part I)*; World Scientific: 1995, pp 155–192.

(14) Dreuw, A.; Head-Gordon, M. *Chemical reviews* **2005**, *105*, 4009–4037.

(15) Granucci, G.; Persico, M.; Zoccante, A. *The Journal of chemical physics* **2010**, *133*, 134111.

(16) Nelson, T.; Fernandez-Alberti, S.; Roitberg, A. E.; Tretiak, S. *The Journal of chemical physics* **2013**, *138*, 224111.

(17) Hammes-Schiffer, S.; Tully, J. C. *The Journal of chemical physics* **1994**, *101*, 4657–4667.

(18) Pittner, J.; Lischka, H.; Barbatti, M. *Chemical Physics* **2009**, *356*, 147–152.

(19) Werner, U.; Mitrić, R.; Suzuki, T.; Bonačić-Kouteck, V. *Chemical Physics* **2008**, *349*, 319–324.

(20) Ryabinkin, I. G.; Nagesh, J.; Izmaylov, A. F. *The journal of physical chemistry letters* **2015**, *6*, 4200–4203.

(21) Plasser, F.; Ruckenbauer, M.; Mai, S.; Oppel, M.; Marquetand, P.; González, L. *Journal of chemical theory and computation* **2016**, *12*, 1207–1219.

(22) Helgaker, T.; Jorgensen, P.; Olsen, J., *Molecular electronic-structure theory*; John Wiley & Sons: 2014.

(23) Valiev, M.; Bylaska, E.; Govind, N.; Kowalski, K.; Straatsma, T.; Van Dam, H.; Wang, D.; Nieplocha, J.; Apra, E.; Windus, T.; de Jong, W. *Computer Physics Communications* **2010**, *181*, 1477–1489.

(24) Kenny, J. P.; Janssen, C. L.; Valeev, E. F.; Windus, T. L. *Journal of computational chemistry* **2008**, *29*, 562–577.

(25) Barbatti, M.; Ruckenbauer, M.; Plasser, F.; Pittner, J.; Granucci, G.; Persico, M.; Lischka, H. *Wiley Interdisciplinary Reviews: Computational Molecular Science* **2014**, *4*, 26–33.

(26) Balasubramani, S. G.; Chen, G. P.; Coriani, S.; Diedenhofen, M.; Frank, M. S.; Franzke, Y. J.; Furche, F.; Grotjahn, R.; Harding, M. E.; Hättig, C., et al. *The Journal of chemical physics* **2020**, *152*, 184107.

(27) Furche, F.; Ahlrichs, R.; Hättig, C.; Klopper, W.; Sierka, M.; Weigend, F. *Wiley Interdisciplinary Reviews: Computational Molecular Science* **2014**, *4*, 91–100.